

Enhancing Organic Photovoltaics with Gold Nano-Particles

A MAJOR QUALIFYING PROJECT

Submitted to the Faculty of the

Worcester Polytechnic Institute

In partial fulfillment of the requirements for the

Degree of Bachelor of Science

By

Nathan Nesbitt

Daniel Nuzzo-Mueller

Date: April 21, 2011

Dr. Nancy A. Burnham, Co-Advisor

Dr. Christopher Lambert, Co-Advisor

I. Contents

Enhancing Organic Photovoltaics with Gold Nano-Particles.....	i
I. Contents	iii
II. Abstract	vi
III. Executive Summary	vii
Chapter 1. Introduction	1
Chapter 2. Literature Review	7
2.1 Photosynthesis – A Background	7
2.2 Organic solar cell overview	13
2.2.1 Grätzel Construction	15
2.2.2 How a Grätzel Works.....	16
2.2.3 Current Advances with Grätzel Dyes	17
2.3 Electrolytes	18
2.4 Increasing stability	20
2.5 Thin Film Systems	20
2.6 Testing Procedures.....	26
2.7 Effects of Surface Topography on Efficiency	27
2.7.1 Electrical and Topographic AFM	27
2.7.2 Titanium Dioxide Nanotube Arrays.....	30
2.7.3 Donor Acceptor Heterojunction Morphology.....	32

2.7.4	Porphyrins on Gold Nano-Particles	36
2.7.5	Summary of the Effects of Surface Topography	38
Chapter 3.	Methods Chapter	46
3.1	Introduction	46
3.2	Grätzel Cell	46
3.2.1	Construction	46
3.2.2	Difficulties	51
3.3	Thin-Film Solar Cell	52
3.3.1	Thin-Film Solar Cell Construction	52
3.3.2	Difficulties	54
3.4	Rough Surface Construction	55
3.5	Photoelectrochemistry Set-up	57
3.5.1	Final Set-up	57
3.5.2	Set-up Problems Encountered & Trouble Shooting	61
3.5.3	Three Electrode Potentiostat Set-up	62
3.6	Surface Characterization	63
3.7	Atomic Force Microscopy	65
Chapter 4.	Results & Discussion	71
4.1	Results	71
4.1.1	Light Absorbance	71

4.1.2	Contact Angles.....	73
4.1.3	Filtering the Irradiation.....	75
4.1.4	Photobleaching.....	75
4.1.5	AFM Topography	76
4.1.6	Photovoltage and Photocurrent.....	78
4.2	Discussion.....	80
4.2.1	Light Absorbance.....	80
4.2.2	Contact Angles.....	81
4.2.3	Filtering the Radiation	82
4.2.4	Photobleaching.....	82
4.2.5	AFM Topography	82
4.2.6	Photocurrent and Photovoltage.....	85
Chapter 5.	Summary & Recommendations	87
5.1	Summary.....	87
5.2	Recommendations.....	87
5.2.1	Improving the Gold Nano-Particle Rough Surface.....	87
5.2.2	Developing a Commercially Viable Solar Cell	89

II. Abstract

Thin-film organic solar cells offer an inexpensive and environmentally friendly alternative to semiconductor solar cells. Despite potentially high quantum efficiency, thin-film cells have low light-absorption compared to semiconductor variants. To increase absorption we deposited gold nano-particles onto the thin-film substrates, increasing the surface area for light harvesting molecules. Photocurrent measurements taken with a lock-in amplifier increased by approximately 50% with addition of the nano-particles. Such improvements could make photovoltaics more cost competitive with fossil fuels and help mitigate climate change.

III. Executive Summary

A number of organizations, including the Intergovernmental Panel on Climate Change, the United States Army, and the World Bank have officially recognized that burning of fossil fuels by humans has caused an increase in the concentration of carbon dioxide (CO₂) in our atmosphere (Glenn, Gordon, & Florescu, 2009), (Alley et al., 2007). This has fueled an increase in the average temperature of Earth by 0.74 ± 0.18 °C, which threatens many ecosystems and the stability of our society. The New Rules Project (NRP) and has shown that the use of renewable energy technology can solve this problem by replacing the burning of fossil fuels (Farrell & Morris, 2010). Unfortunately, as shown by Economics for Equity and Environment, this would be very expensive to do (Ackerman *et al.*, 2009). Photovoltaic technology is a large part of the renewable energy portfolio suggested by the NRP, but is also the most expensive type of renewable energy technology that NRP analyzed (it is almost double the cost per MWh of the second most expensive renewable energy technology, concentrated solar). This demonstrates an important niche for the development of low-cost photovoltaics.

Organic solar cells offer an inexpensive and environmentally friendly alternative to silicon photovoltaics, the predominant photovoltaic panel commercially in use today. Organic solar cells consist of a metallic or semiconductor substrate onto which organic dye molecules are adsorbed. An electrolyte is present above the dye molecules, which provides an electrical connection to a counter-electrode. An oxidizing or reducing agent in the electrolyte provides the driving mechanism for current, as it will either act as an oxidant or reductant to the dye molecule when the dye is in an excited state. The process for generating photovoltage and photocurrent is as follows for an electrolyte with an oxidant: a photon from incident irradiation is absorbed by a

dye molecule, putting the dye molecule in an excited state with a higher reduction potential than before excitation. The dye molecule is then oxidized by the oxidant, removing an electron from the dye molecule and injecting it into the electrolyte solution. This drives oxidation of methyl viologen at the counter electrode thereby transferring an electron to the counter electrode and giving it a net negative charge. To restore its electron shells, the dye molecule pulls an electron from the primary electrode, which gives the primary electrode a net positive charge. This charge build up on the electrodes is responsible for the photovoltage between the electrodes, and the photocurrent when the two electrodes are connected. For a reducing agent in the electrolyte solution, the mechanism is the same, but the polarization of the cell is reversed.

Unfortunately, organic solar cells are presently limited by their efficiency and their stability. Grätzel cells are a common type of organic solar cell which have a porous semiconductor substrate that dye molecules adsorb to. This provides a thick layer of dye molecules, and thus high absorption of incident light. However, the disorder in the molecules makes side reactions more likely. This decreases the stability of the cell and limits conversion of excitation energy in the dye molecules to photocurrent. Thin-film solar cells are another common organic solar cell which have a metallic or semiconductor substrate covered in a self-assembled monolayer (SAM) that terminates in the dye molecules. Thin-film solar cells have the potential to be more stable than Grätzel cells because of the well ordered structure the SAM provides. This order should reduce undesired side-reactions, which prevents cell degradation and increases conversion of excitation energy to photocurrent. However, because the dye molecules are in a monolayer, the layer of them on the substrate is very thin, which causes very low absorption of light.

To address the low absorption of thin-film solar cells, the use of gold nano-particles to roughen the surface of the metallic substrate was investigated. The rough surface should increase the surface area of the cell and thereby the density of the dye molecules and the absorption of irradiation. The concern with this approach is that the rough surface could introduce disorder that would reduce the efficiency of the cell.

The construction of a thin-film solar cell involves a sequence of baths to develop the monolayer on the primary electrode. The process starts with a glass slide covered with a smooth thin layer of gold. This is cleaned and placed in a bath of linking molecules, which form a SAM on the gold surface. The slides are then placed in a bath of dye molecules, which adsorb to the exposed surface of the monolayer. These slides are removed from solution and rinsed to create a complete electrode. The complete electrode is then placed in an electrolyte solution with an oxidizing agent and a counter electrode to create a complete solar cell for testing. To make the gold surface rough, the clean gold covered glass slide is first put in a bath of linking molecules, then a bath of gold seed particles, and finally a bath of gold nano-particle growth solution. After the nano-particles are grown, dye molecules are adsorbed to the gold to create a complete solar cell as previously described.

A number of methods were used to characterize the primary electrode of the thin-film solar cells studied. Absorption spectra were taken of the smooth and the rough surfaces to determine which molecules absorbed light and whether the rough surface provided an increase in absorption. Atomic force microscopy (AFM) was used to characterize the topography of the surface and measure the increase in surface area. A self-made photonics setup with a lock-in

amplifier was used to measure the photovoltage and photocurrent of the cells and determine their ultimate efficiency.

Two batches of smooth and rough electrodes were made for characterization, labeled Batch 1 and Batch 2. AFM images of Batch 1 showed a substantial difference between the smooth and rough surfaces, with good nano-particle coverage on the rough electrode. Batch 2 showed little difference between the smooth and rough surfaces, with little nano-particle coverage on the rough electrode. Measurements of the absorption, the photovoltage, and the photocurrent were consistent with the AFM images, showing an increase for rougher surfaces. In Batch 1, the photovoltage and photocurrent increased by approximately 50%. This suggests our hypothesis is correct, that addition of gold nano-particles to roughen the substrate's surface is an effective way to inexpensively and with little difficulty increase the performance of thin-film organic solar electrodes. To incorporate this into commercially viable solar cells, a cell design must be developed which will further increase the power output by approximately a factor of 1000, and thus make it comparable to existing solar cell technology. With the development of such a design, organic thin-film solar cells could offer a type of solar cell technology that is more cost effective and environmentally friendly than silicon photovoltaics and help solve the issue of rapid global climate change.

In future work more data sets can be acquired to demonstrate repeatable synthesis of the rough gold nano-particle surface and to confirm the increase in photovoltage and photocurrent with the addition of these particles. A variety of experiments can be done to better understand the topography of the nano-particle surface, how the topography affects the absorption of irradiation, and how the surface can then be optimized. Design of a commercially viable solar cell would be the ultimate end of this work.

References

- Alley, Berntsen, Bindoff, Chen, Chidthaisong, Friedlingstein, et al. (2007). *Climate change 2007: Working group I: The physical science basis* No. 3) Intergovernmental Panel on Climate Change.
- Farrell, J., & Morris, D. (2010). *Energy self-reliant states, updated may 2010* Institute for Local Self Reliance.
- Frank Ackerman, Elizabeth S. Stanton, Stephen J. DeCanio, Eban Goodstein, Richard B. Norgaard, Catherine S. Norman, Kristen A. Sheeran. (2009). The economics of 350: The benefits and costs of climate stabilization. *Economics for Equity and the Environment: E3 Network*,
- Glenn, Gordon, & Florescu. (2009). *2009 state of the future* The Millennium Project.

Chapter 1. Introduction

Organizations such as the Intergovernmental Panel on Climate Change (IPCC), the United States Army, and the World Bank have officially recognized that burning of fossil fuels by humans has caused an increase in the carbon dioxide (CO₂) concentration of our atmosphere and has fueled an increase in the average temperature of Earth. The concentration is currently 385 ppm, 35 ppm above the highest safe concentration predicted by climate scientists (Hansen, 2008). Without the replacement of fossil fuel sources with renewable alternatives, the concentration will remain above 350 ppm and cause an irreversible increase in temperature; tipping points such as the melting of glacial ice caps make this temperature increase permanent and drive positive feedback loops causing further warming. Damage to our environment will include ocean acidification, loss of fresh water supplies, and shifting climatic zones.

Technology that could replace fossil fuels as society's primary source of energy already exists. For example, 86% of the states in the USA could generate all of their electricity by covering less than 1% of their land area with amorphous silicon photovoltaics (Farrell & Morris, 2010). Looking only at the land area provided by rooftops, many states could generate at least 20% of their electricity and states like California and Nevada over 50%. Unfortunately, the existing renewable energy sources are expensive. It is estimated that it would take between 2 and 8 years to recoup their investment (Bankier & Gale, 2006) (Current estimates show it would cost about 2.5% of the global Gross Domestic Product (GDP) to reach 350 ppm of CO₂ by the end of the century. This is equivalent to one year of typical GDP growth for most developed countries (Frank A. et al, 2009). Existing renewable energy sources also involve materials that are either

scarce or harmful to the environment. For example, wind turbines use rare earth magnets and the production of amorphous silicon photovoltaics uses many toxic chemicals.

Thin-film organic solar cells, which often use porphyrin dye molecules similar to chlorophyll from the photoreaction center in plants, are cheap and do not require harmful materials. They are seeing an introduction now in low-energy demand applications such as backpacks with built in solar panels (Plastic Electronics). The molecular order provided by their monolayer structure also affords a high quantum yield, in which 95% percent of the absorbed photons contribute to the production of useful electricity (Sarovar M. et al, 2010). To make them commercially viable, however, their molecular stability must be improved to extend the lifetime of the panels, and their absorption of photons must be increased to improve their energy output per unit area.

Instability in organic solar cells is caused by the high reactivity of the pigment molecules when their electrons are excited by incoming light. This reactivity causes side-reactions that degrade the cell. Plants are able to avoid this because of the high degree of order in the molecular structure of their photoreaction center, as seen in Figure 1, which allows the chlorophyll to discharge their electron in the range of picoseconds, and allows them to avoid degradation of the chlorophyll. It is hoped that with further research it will be possible to mimic plants in this regard. This order allows an excited electron to leave the pigment molecule quickly, and prevent charge recombination or side-reactions prolonging the life of the cell. Thin-film solar cells have their pigment molecules in a monolayer structure, which provides order similar to that of plants. However, further improvement of this structure is required to achieve the same stability accomplished by plants.

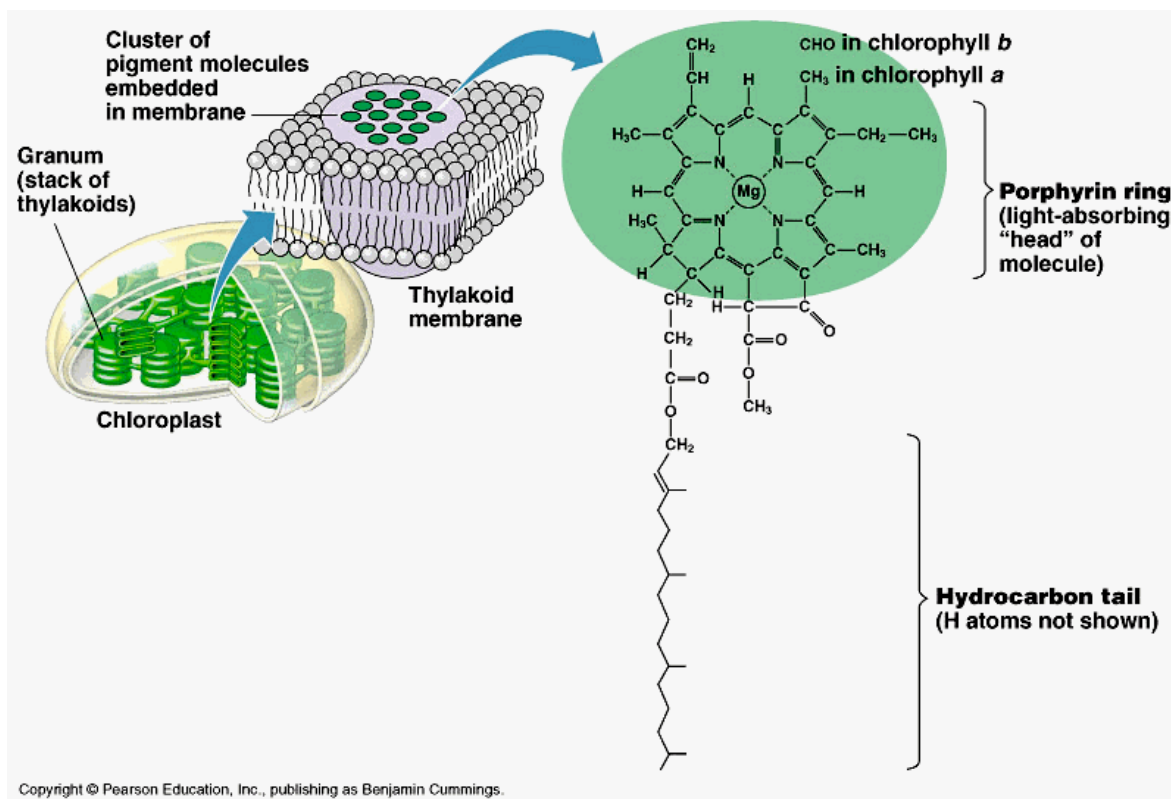


Figure 1 (Pearson Education Inc.): Porphyrins are part of a cluster of organic molecules that are embedded in the cell membrane. Their orientation and ordering inside of the membrane allow them to discharge their electrons before the photosensitive porphyrin reacts with other nearby molecules, causing the porphyrin to degrade.

Low absorption of incident photons by thin-film photocells is caused by the monolayer structure of the pigment molecules. This structure makes the photoreactive part of the thin-film photocell much thinner than an amorphous silicon photovoltaic cell, which limits the amount of light absorbed.

Thus we seek to increase the absorption of the thin film solar cell while maintaining the appropriate monolayer structure necessary for a high degree of molecular order. In this project we will increase the per unit area density of the porphyrins in the film by roughening the surface of the gold substrate as seen below in Figure 2. This will allow more porphyrins to be attached to

a given gold substrate. This approach could increase the cell's efficiency for a negligible increase in the production cost and difficulty. However, roughening by adding spheres can only increase the light absorption by a factor of two. Due to the fact that light absorption is at less than 1% for current smooth cells, this research will only provide a scientific base to confirm whether roughening the cell's electrode does in fact increase photovoltage and photocurrent. This research would have to be combined with further research into developing these cells to produce a viable alternative to silicon photovoltaics.

A potential issue with the rough surface is that it could place adjacent porphyrins at different heights, which could lead to excited electrons being transferred between adjacent porphyrin molecules or to the MUA monolayer, rather than being injected into the electrolyte. This transfer could cause the molecules to degrade at an accelerated rate making the solar cells impractical; even smooth thin-films become inoperable after several months of use.

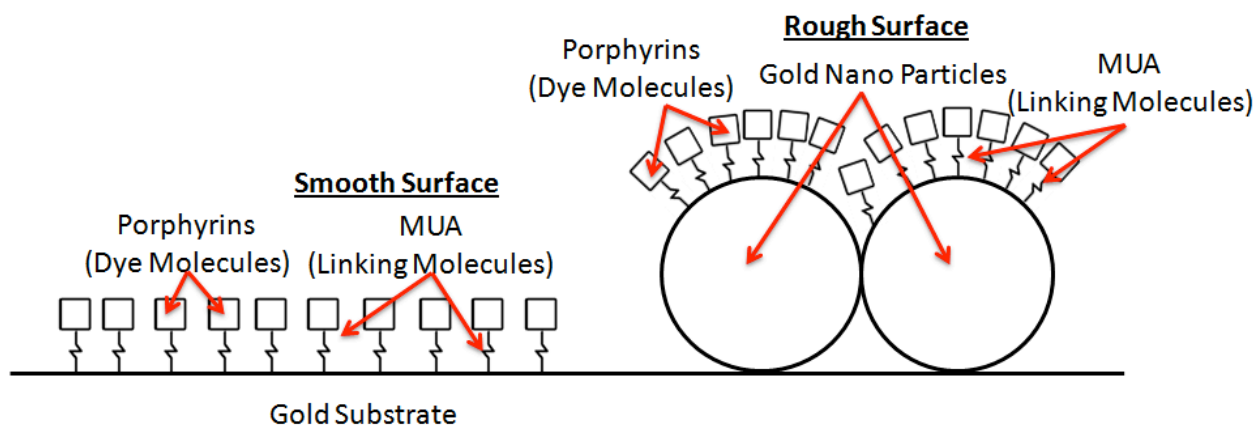


Figure 2: A rough surface will allow more porphyrins to fit onto a single substrate because the porphyrin heads can exist at different heights and crowd closer together.

To determine whether a rough surface will allow for greater photovoltage and photocurrent, a rough and smooth electrodes will be used for the same solar cell design for comparison. The electrode surface will be roughened by adding gold nano-particles to the surface. The absorption spectrum of the surface will be measured to determine the wavelengths of light that are being absorbed by the cell. To determine the topography of the substrates, Atomic Force Microscopy will be used. Finally, the photovoltage and photocurrent produced by the cell will be measured using a lock-in amplifier. This will provide a correlation between the efficiency of the thin film with the substrate's roughness.

This MQP report is structured as follows: Introduction, Literature Review, Methods, Summary and Recommendations. The introduction gives background into the experiment , its goals, and the problem it hopes to address. The literature review goes over current knowledge that surrounds the issue and other experiments that have been done concerning similar technologies and research. The Methods section outlines the experimental procedure that we followed in order to produce our results. These results presented and analyzed in the Results and Discussion. Summary and Recommendations reviews the findings of this project and suggests possible directions in which the work could be expanded upon in further research.

References

- Hansen, James. "Target Atmospheric CO₂: Where should Humanity Aim?" *Open Atmospheric Science Journal* 2, (2008).
- Farrell, John, and David Morris. *Energy Self-Reliant States, Updated may 2010*. Institute for Local Self Reliance, 2010.
- Frank A., Elizabeth S. S., Stephen J. D., Eban G., Richard B. N., Catherine S. N., Kristen A. S. "The Economics of 350: The Benefits and Costs of Climate Stabilization." *Economics for Equity and the Environment: E3 Network* (2009).
- Sarovar, M., *et al.* "Quantum Entanglement in Photosynthetic Light-Harvesting Complexes." *Nature Physics* 6.6 (2010): 462-7.
- Pearson Education Inc., "Photosynthesis." <http://kentsimmons.uwinnipeg.ca/cm1504/photosynthesis.htm>
- Bankier, C., & Gale, S. (2006).
Energy payback of roof mounted photovoltaic cells. *Energy Bulletin*,
- Plastic Electronics, "First commercial product for organic solar cell"
<http://www.plusplasticelectronics.com/Energy/First-commercial-product-for-organic-solar-cell.aspx>

Chapter 2. Literature Review

2.1 Photosynthesis – A Background

The system that plants and photosynthetic bacteria have developed for converting incident light energy into charge separation has a high quantum yield of 95% (Scheuring & Sturgis, 2009), (Pullerits & Sundstrom, 1996) which has inspired substantial research into the replication of this system for the development of inexpensive solar cells. This first section is a short review of the photosynthetic process found in nature, the high quantum yield of which we seek to emulate in the design of organic solar cells. The process of photosynthesis begins with photoexcitation of photosensitive dye molecules, followed by the creation of a charge separation. This provides energy for the production of nicotinamide adenine dinucleotide phosphate (NADPH) and adenosine triphosphate (ATP), essential energy carrying molecules for the life processes in living organisms. Photosynthesis accomplishes this charge separation through a complicated process involving the reaction of many different molecules. Our solar cell design will attempt to use the most basic component of this process, an organic light sensitive dye molecule, to convert incident light energy into charge separation in a photosensitive film deposited on a gold substrate.

Purple photosynthetic bacteria are a popular focus for research of photosynthesis because they carry out a particularly simple photosynthetic process (Scheuring & Sturgis, 2009). The cell has two lipid bi-layer membranes, an outer one that encloses the cell, and an inner one embedded with photosynthetic proteins. There are two different molecular complexes that capture the energy of incident light, light harvesting complex 1 (LH1) and light harvesting complex 2 (LH2). The energy captured by these proteins is sent to another protein complex, the reaction center,

where it is used to create a charge separation. The energy stored in this charge separation is used by other proteins to generate Adenosine Triphosphate (ATP), as described in Figure 3.

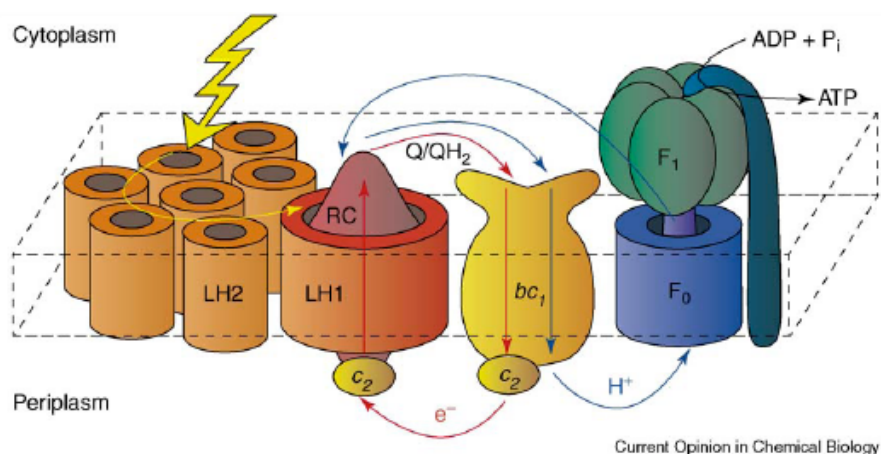


Figure 3 (Scheuring, 2006): **Photosynthetic protein complexes embedded in the inner cell membrane of purple bacteria. Photosensitive antennas in light-harvesting complex 1 and 2 (LH1 and LH2) absorb photons and transfer the excitation to the reaction center (RC). The RC is contained inside of LH1, and produces a free electron from the excitation. The electron is transferred to a quinone, and after the quinone accepts two electrons the resulting quinol (QH₂) is oxidized by cytochrome c₂. This reaction is catalyzed by cytochrome bc₁ (bc₁), and drives the proton gradient between the cytoplasm and periplasm. F₀F₁-ATP-Synthetase uses the proton gradient to generate ATP from ADP and inorganic phosphate. The yellow arrows represent excitation-transfer, the red arrows electron-transfer, and the blue arrows proton-transfer.**

Slightly different pigments are used to capture incident light energy than to gather excitation energy and generate a charge separation. Barber and Archer studied the pigments that fill these roles for plants (Barber & Archer, 2001). In plants the roles are filled by several different kinds of chlorophyll: antenna chlorophyll to capture incident light energy, and two different complexes of chlorophyll *a* to generate the charge separation. The two complexes of chlorophyll *a* are P680 and P700, named for their peak absorption wavelengths. These two complexes of chlorophyll *a* have different surrounding proteins in the thylakoid membrane

which give them a different electronic structure and consequently different absorption spectra (Anestis, 2006).

Plants have two photosystems, photosystem I and photosystem II, which operate in sequence to carry out photosynthesis. Each photosystem is composed of the basic components described for the purple photosynthetic bacteria, a system of light harvesting complexes and a reaction center. To generate a charge separation each photosystem has a type of chlorophyll *a* in the reaction center, P700 for photosystem I P680 for photosystem II.

When light is absorbed by any of the pigment molecules in photosynthetic organisms, it puts the molecules in an excited state in which there is an electron-hole pair, or an exciton (Govindjee & Coleman, 1990). This exciton travels across the adjacent pigment molecules to reach the reaction center, where it is absorbed by P680. P680 has a red absorption peak that is a longer wavelength than the peak for the antenna chlorophylls (Barber & Archer, 2001). This makes P680 a trap for excitons that are generated near it and transferred to it. When pigment molecules are excited they become more reactive and better oxidizing and reducing agents. When P680 is excited it acts as a reducing agent and donates an electron to a nearby electron acceptor in the reaction center, pheophytin (Pheo). This donation makes P680 a strong oxidizing agent and allows it to strip electrons from oxygen with the help of catalysts in the reaction center.

Stripping an electron from oxygen with P680 is the start of the charge separation process in photosynthesis. This process proceeds to take steps to build distance between the positive and negative charges to ensure that they do not recombine and waste the energy stored in their separation. In this process Pheo passes the electron it accepted from P680 to another electron acceptor, quinone Q_A , which likewise passes the electron to quinone Q_B . Quinone Q_B accepts two protons in addition to the electron, and diffuses to another stage in the photosynthetic process for

the generation of NADPH and ATP (Szalai, 1998). The creation of the charge separation and the development of distance between the charges are outlined in Figure 5. This entire process is facilitated by many specialized polypeptides and proteins in the photosystem (Govindjee & Coleman, 1990), which makes the process impractical to try and imitate in artificial solar cells. For our thin film solar cells our primary photosensitive dye will be a porphyrin molecule similar to the porphyrin group that is in chlorophyll. An electrolyte with methyl viologen as an oxidizing agent serves as an electron acceptor to create a charge separation after photoexcitation of the porphyrin occurs. Figure 4 shows this porphyrin and chlorophyll *a*.

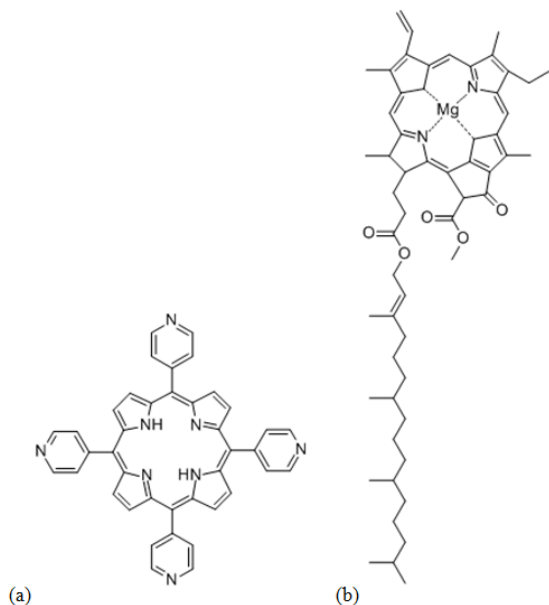


Figure 4 (Sharma, Broker, Szulczewski, & Rogers, 2000a): **(a) Porphyrin (meso-Tetra (4-pyridyl) porphine) ($C_{40}H_{26}N_8$)**, the pigment used to photosensitize our organic solar cells. **(b) Chlorophyll a ($C_{55}H_{72}O_5N_4Mg$)**, a primary pigment in photosystem II in plants.

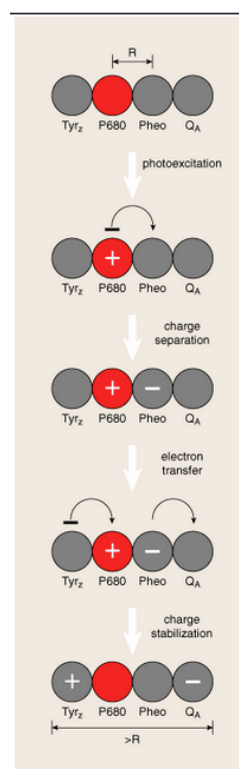


Figure 5 (Szalai, 1998): **The process by which an exciton is developed into a charge separation, and the charges are placed far from one another to prevent recombination and loss of the stored energy.**

Use of Atomic Force Microscopy (AFM) and electron crystallography have provided insight into the structure of LH1, LH2, and RC, and into how the excitation energy captured from incident light is used to create a charge separation. One way AFM was used to provide this insight was to characterize the surface topography of the protein complexes in LH1, LH2 and the reaction center. In particular, the internal structure and placement of the LH1, LH2 and the reaction center within the inner membrane of purple photosynthetic bacteria was studied through AFM (Scheuring & Sturgis, 2009). This characterization has shown that the light harvesting complexes are made of rings of proteins as shown in a schematic in Figure 3 and an AFM image in Figure 6. AFM is especially valuable for imaging these surfaces because the high signal to noise ratio avoids any need to average or make ensemble measurements and thereby alter the protein structure or placement within the cell (Scheuring & Sturgis, 2009). AFM and electron crystallography of the RC and the surrounding LH1 found in plants have revealed a backbone protein structure of long transmembrane helices, arranged in a ring as seen in Figure 7 (Barber & Archer, 2001), (Scheuring & Sturgis, 2009). These helical proteins provide the framework for β -carotenoid, chlorophyll, and pheophytin, the three primary photosensitive dye molecules found in LH1, LH2, and RC of plants. These pigment molecules are held in the center of the ring in arrangements that benefit photoexcitation for LH2, and charge separation for LH1 and RC. Electron crystallography of LH1 and RC determined the placement of the P680 (a type of chlorophyll) and pheophytin within the RC, as shown in Figure 8 (Barber, 2001). As with the specialized proteins and polypeptides involved in the chemical process of charge separation, the intricate framework of the pigment molecules in the reaction center is impractical to artificially generate. However, the high quantum yield of this system motivates an understanding of it for the design of pigment orientation in artificial organic solar cells. Our arrangement uses only a

porphyrin molecule for photoexcitation, which is anchored to a self-assembled monolayer on a metallic substrate, as described in the following section.

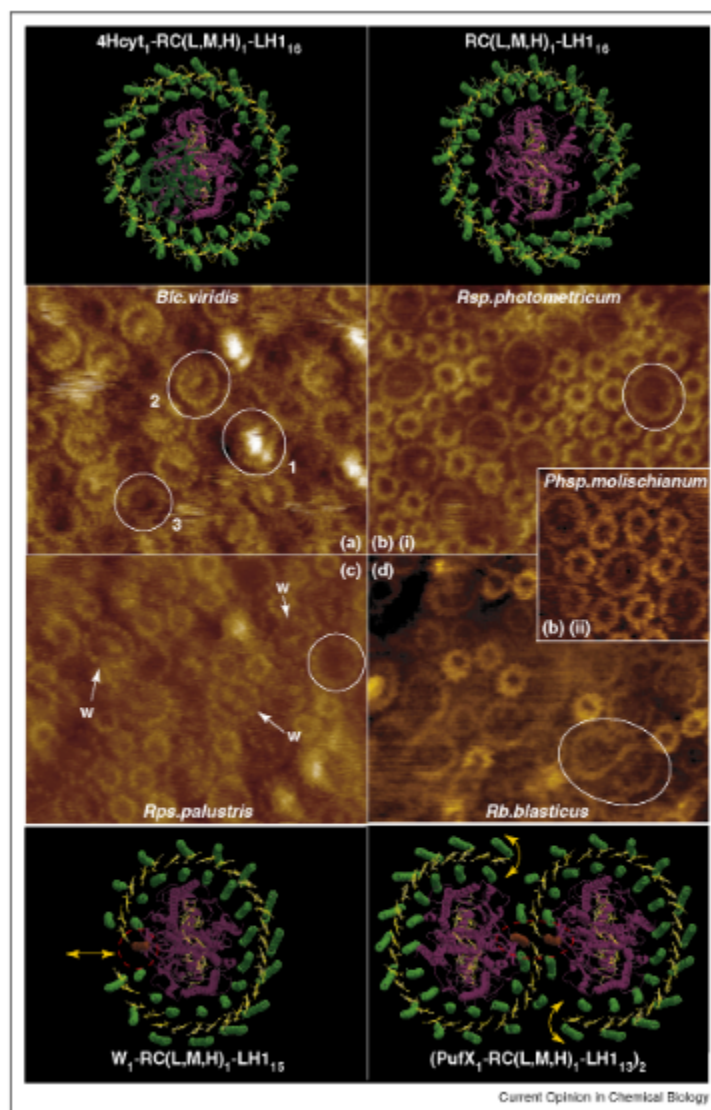


Figure 7 (Barber & Archer, 2001): AFM images of the inner membrane of four species of purple photosynthetic bacteria (center), and computer generated renditions of the molecular composition of the LH1, LH2 and reaction center (RC). The rings in the AFM images are the cross-membrane helical proteins that provide the framework for these protein complexes. In the top and bottom renditions, the helical cross-membrane proteins are green, the RC subunits are purple, and the gates for the quinone Q/QH₂ are marked with yellow arrows.

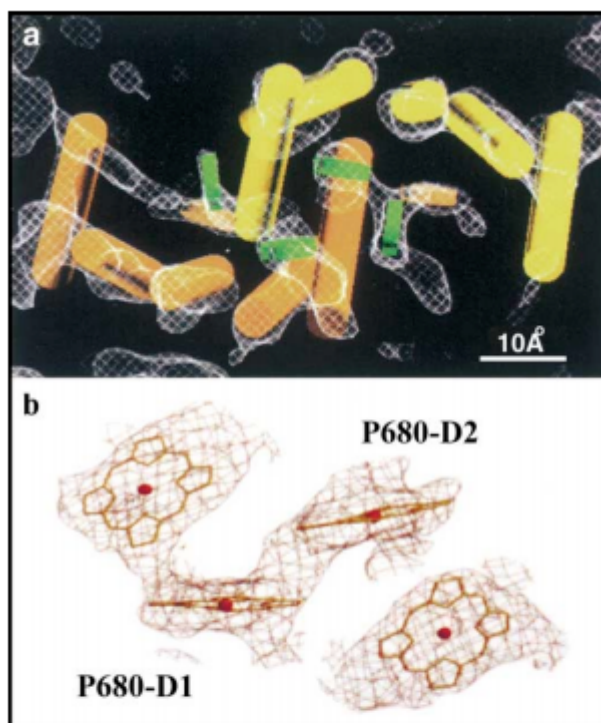


Figure 8 (Barber & Archer, 2001): **(a)** Positioning of the four ‘core’ chlorophylls (green) within the D1 (yellow) and D2 (orange) transmembrane helices. The data were obtained by electron crystallography. **(b)** Positioning of the four ‘core’ chlorophylls of P680 as determined by X-ray crystallography.

2.2 Organic solar cell overview

There has been a good deal of research into the adaptation of these photosynthetic mechanisms to develop viable photocells (Uosaki & Kohei, 1997). Currently, most photocells under large scale production are based on a semi-conductor p-n junction system in order to produce useable wattage from light (Grätzel, 2003). One method to reproduce the photosynthetic mechanisms of plants is the use of Grätzel cells and thin film photocells. These cells have an advantage over current semi-conductor photocells because they are roughly 10-20% the cost (Grunwald & Tributsch, 1997). The efficiency of organic solar cells would make them a viable alternative to silicon based solar cells because the efficiency of a Grätzel cell is

roughly half that of a silicon cell but its cost can be roughly 5-10 times less. This makes them a less expensive alternative to current silicon options. When comparing the efficiency of the thin-film versus the Grätzel cell, it is insightful to consider the difference between incident photon to current efficiency (IPCE), absorption, and quantum efficiency. A thin film system has a high quantum efficiency, which means it converts absorbed photons into excited electrons very efficiently. However, it has much lower absorption than a Grätzel cell because its thinness makes it so transparent. This suggests that thin-film cells may have more potential if their absorption can be improved.

The Grätzel cells are based on having a dye absorb the energy from incident light and transfer it through a circuit much like a solar cell. Changing the dye in these cells gives them different absorption spectra. As such, the efficiency is wavelength dependant, and each type of dye gives the cell a different efficiency spectrum. The dye essentially acts as a light activated voltaic cell that absorbs photons and causes a potential difference.

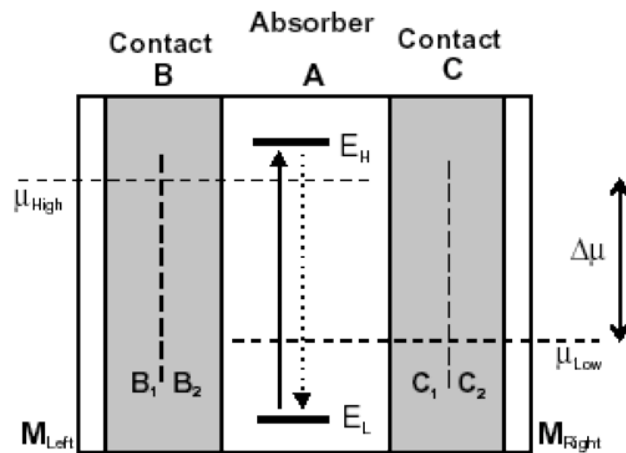


Figure 9 (Bisquert, Cahen, Hodes, R \tilde{A} / \hbar le, & Zaban, 2004): **Diagram of the mechanism for a Grätzel cell. Contact B acts as the high voltage side of the voltage and Contact C acts like the low voltage side. The absorber is responsible for increasing the energy level of the electrons and causing a voltage differential across the two.**

2.2.1 Grätzel Construction

To construct Grätzel cells two layers of conducting glass are taken and one is coated with a wide-band gap semi-conductor. Then a dye is adsorbed onto this semiconductor layer. The second piece of conducting glass is placed on top of the first and an electron donor solution is added between these layers.

The wide band gap oxide semiconductor used in Grätzel's original cell was TiO_2 . A thin layer of this is placed onto the slide and then it is sintered in order to produce a crystalline structure. The slide is then immersed in a solution of the dye and left to soak. This allows the dye particles to attach to the TiO_2 layer.

2.2.2 How a Grätzel Works

When light of a wavelength that matches a step in the dye's energy levels is absorbed by the dye molecule in the cell, electrons flow down a potential gradient from the higher voltage at the TiO_2 layer, the cathode, to the lower voltage at the other conducting glass slide, the anode. The electrolyte, which has a reducing agent in it, facilitates this electron flow through reduction of the dye by the reducing agent. A reduction reaction is a reaction in which the reducing agent gives an electron to another molecule thereby reducing the other molecule and oxidizing itself. This reduction reaction prevents the dye molecule from undergoing radiationless decay to the dye molecule's ground state. Ideally, this reduction reaction happens within picoseconds to ensure that radiationless decay or side-reactions do not occur (Grätzel, 2003).

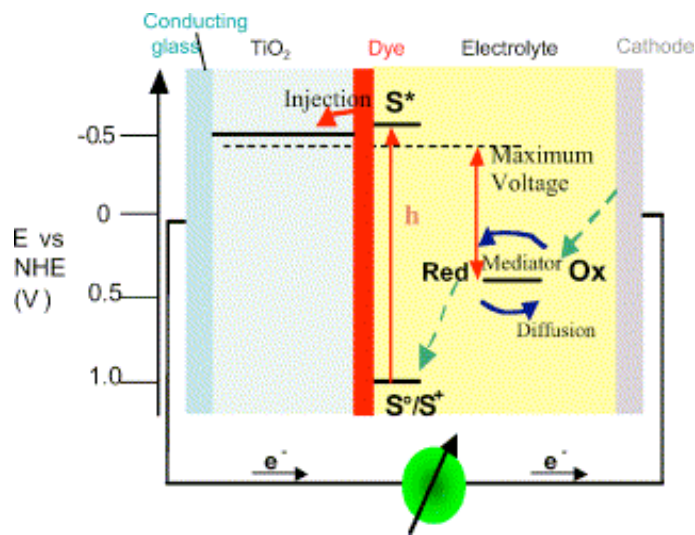


Figure 10 (Grätzel, 2003): When light strikes the dye in the Grätzel cell an electron is injected into the TiO_2 layer and quickly replaced by an electron from the electrolyte. From the TiO_2 there is electron flow through the circuit which results in charge passing from the cathode into the electrolyte to complete the circuit.

2.2.3 Current Advances with Grätzel Dyes

The field of advances with Grätzel cells is related mainly to the choices and construction of new dyes to be used with the system. Currently one of the most effective dyes is N3 (tri(cyano)-2,2',2''-terpyridyl-4,4',4''-tricarboxylate)Ru(II)). This dye allows for a 10.4% efficiency of the cell (Grätzel, 2003); research into ruthenium dyes is expected to yield up to 15% efficiency. See Figure 11 for the chemical structure of N3 dye and Figure 12 for the absorption spectra.

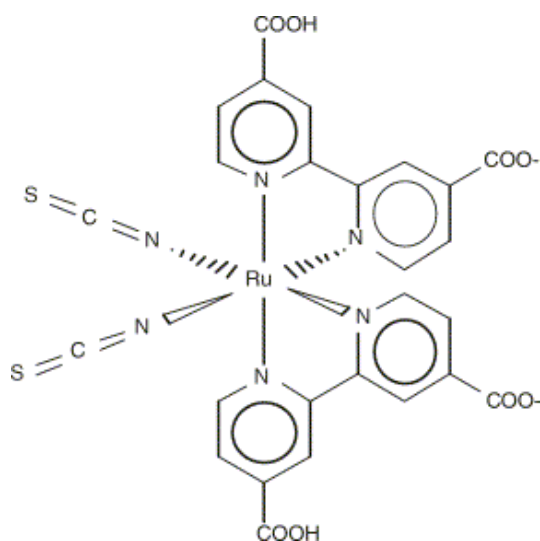
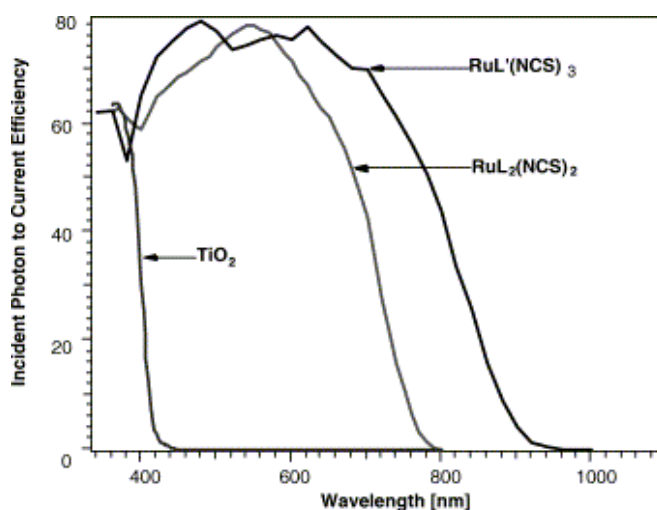


Figure 11 (Grätzel, 2003): Chemical structure of N3 dye used by Michael Grätzel



L = 4, 4'-COOH-2,2'-bipyridine
L = 4,4',4'' -COOH-2,2':6',2''-terpyridine

Figure 12 (Grätzel, 2003): Incident photon to current efficiency (IPCE) spectra of TiO₂ and ruthenium based dyes.

There has been discussion about dyes that are based on other molecules and technologies. Grätzel has suggested that research into phthalocyanines, quantum dots, and porphyrins may offer new results (Grätzel, 2003). Each of these has a different absorption spectrum and the use

of them gives efficiencies in different areas of the electromagnetic spectrum. Porphyrins in particular have been experimented with before and efficiencies of around 4% have been reached using them in Grätzel cells (Campbell, Burrell, Officer, & Jolley, 2004). There are many different kinds of dyes other than porphyrins and ruthenium based dyes. The figures demonstrate how different dyes can be used in the production of energy. See Figure 13 for the chemical structure of a porphyrin and Figure 14 for the absorption spectrum. An efficient light absorber will absorb a high percentage of light from a large range of wavelengths. In the case of this porphyrin it absorbs a large amount of light from a very narrow band of wavelengths compared to the N3 dye.

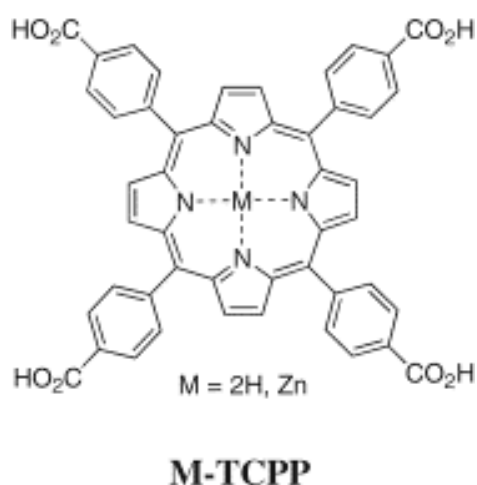


Figure 13 (Campbell *et al.*, 2004): **Chemical structure of porphyrin used by Campbell in porphyrin sensitized TiO₂ cell**

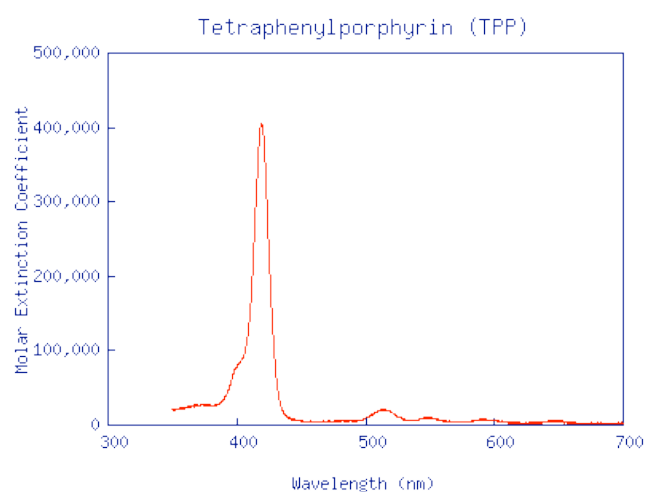


Figure 14 (Prahl, 2011): **Absorption spectrum of a porphyrin**

2.3 Electrolytes

The choice of electrolyte and reducing agent is important to the performance of organic solar cells, and has been a focus of Wang *et al.* and Zhao *et al.* (Wang *et al.*, 2009), (Zhao *et al.*, 2008). Cells are most efficient when the reduction potential of the electrolyte and the ground

state of the dye are most closely matched. Consequently there is a lot of research into finding either a dye that provides a high incident photon to current efficiency (IPCE) which matches the reduction potential of the commonly used iodide/triiodide electrolyte, or finding an electrolyte with a reduction potential that matches the ground state of a desired dye.

The electrolyte is the part of the cell that regenerates the electron in the dye molecule and then receives an electron from the other side of the cell (or *vice versa* depending on the dye and whether a reducing or oxidizing agent is chosen). In this way it completes the circuit between the two slides that make up the cell, acting almost as a “bank” of electrons that are used in the circuit.

Because of this, the electrolyte must be able to efficiently and quickly transfer an electron through the solution once an electron has been excited (Grätzel, 2003). It is therefore typical to use an electrolyte that is a liquid. Since the cells are difficult to seal, evaporation of the electrolyte is a common problem with these cells.

Since solvents have a relatively low vapor pressure they also are more likely to evaporate during use in a solar cell because of the increase in temperature from exposure to the sun. These electrolytes have been found to produce the highest incident photon to current efficiencies seen in these systems, in the range of approximately 10% (Grätzel, 2003).

Another possibility for an electrolyte is the use of ionic liquids (ILs) (Wang *et al.*, 2009). These electrolytes have the advantage of having almost zero vapor pressure and a higher viscosity making them easier to seal in an organic solar cell. These liquids have a noticeably lower efficiency than their volatile counterparts partially because their higher viscosities make it harder for the ions in them to redistribute. This gives around 7% IPCE.

One of the final approaches to creating a very stable electrolyte is the attempt to create a solid electrolyte that can be used in a Grätzel cell (Zhao *et al.*, 2008). Electrolytes have been created from ILs in small-crystalline form and then applied to creating a Grätzel cell. These are the most stable of the electrolytes because they do not require any particular sealing and have no vapor pressure. A drawback is that they achieve IPCE values of only around 2%.

2.4 Increasing stability

There has been research into increasing the stability of Grätzel cells by engineering cells that have different components, which compliment each other's energy levels (Feldt *et al.*, 2010). Because of the unstable nature of the current volatile electrolytes they not only are difficult to seal but also break down metals exposed to them. Side reactions can also be a problem. They occur when excitation energy does not pass quickly enough to the development of charge separation. The result is degradation of the dye molecules, often through oxidation.

Modification of the dye can allow for faster transfer of the electron into the TiO₂ layer (Chen *et al.*, 2009). This prevents the dye from being active too long and beginning to degrade.

There has also been research into using other inorganic dyes such as ones that are cobalt based (Feldt *et al.*, 2010). These types of dye can more efficiently operate with ILs. However, the speed at which an electron is capable of moving out of and into the dye is increased thus making it possible for the electron to move from the TiO₂ layer back into the dye, possibly causing the dye to interact while it is charged. This type of problem has been addressed by using a cobalt mediator to slow down the speed at which dyes can receive and transmit an electron into the TiO₂ layer.

2.5 Thin Film Systems

Recent research into thin film systems is also a growing field (Fujihira, Nishiyama, & Yamada, 1985), (Driscoll *et al.*, 2008). Thin films are based upon the principle of constructing a layer of single molecules or structured molecular systems that cover a surface with only a single layer. These can either be a monolayer or a multilayer where either a single molecule covers the surface or a number of defined molecular structures and are considered organic solar cells along with Grätzel cells.

The research aimed at SAMs in relation to Grätzel cell is because of the desire to mimic the capabilities of photosynthesis (Uosaki, Kondo, Zhang, & Yanagida, 1997). The creation of these systems has been very difficult and has had limited efficiencies using the Langmuir-Blodgett method initially (Fujihira *et al.*, 1985). New methods of forming these SAMs have progressed and they are now significantly easier to produce.

The films being used in our experiments generally are constructed of self-assembling monolayers (SAMs) where the molecules align themselves on the surface by allowing the substrate to be immersed in a bath of the SAM molecules. Further layers can then be added by subsequent baths in other solutions allowing for either the attachment of more of these monolayers in order to create a multilayer system or with a molecule that effectively caps off the thin film.

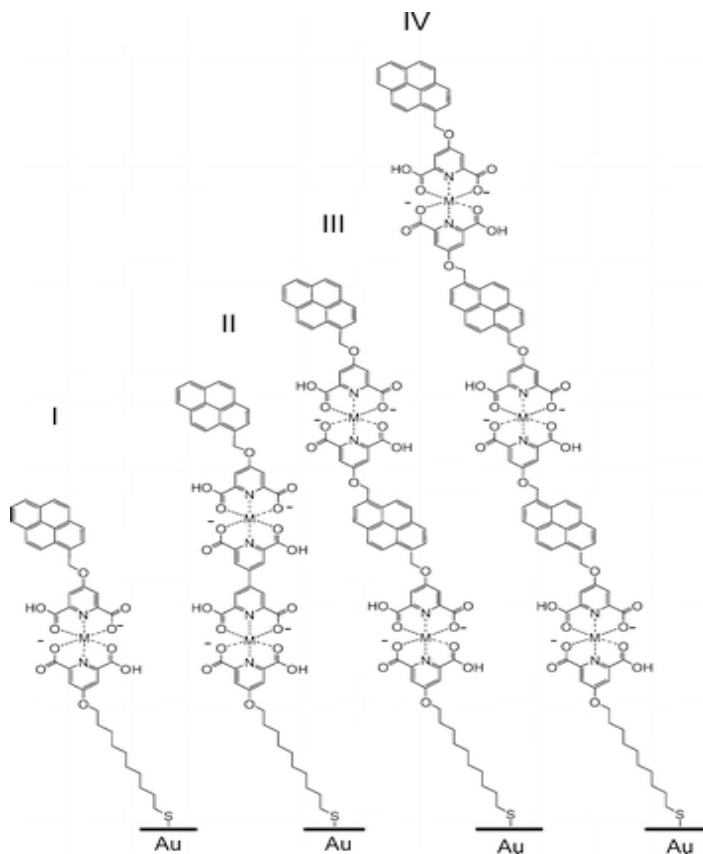


Figure 15 (Driscoll *et al.*, 2008): Monolayers and Multilayers can be built using these SAMs. By layering these dye molecules with linking molecules multilayers of multiple levels can be created. Figure I shows a monolayer where Figures II – IV are examples of multilayers of increasing thicknesses.

Attachment of porphyrins to these SAM molecules has been studied for some time (Sharma, Broker, Szulczewski, & Rogers, 2000b) and there are challenges associated with them such as the binding sites between the initial SAM molecule and porphyrin and the orientation of the porphyrin when they attach to the SAM layer. Molecules can be attached to the SAM layer through many different bonds such as hydrogen bonds (Sharma *et al.*, 2000b) or metal-ligand bonds (Driscoll *et al.*, 2008) or even covalent bonds (Terasaki, Akiyama, & Yamada, 2002). In the case of non-covalent bonds it is easier to construct a complex multi-layer or monolayer due to the fact that it allows for the layer to be constructed block by block rather than needing a

complex molecule to be synthesized and then deposited in a layer. Like Grätzel cells, there has been research towards different types of constructions of these monolayers in order to enhance their ability to transform light into electrical energy (Uosaki *et al.*, 1997).

The attached dyes to the SAMs can also vary greatly. Certain cells use different types of ruthenium based dyes (Terasaki *et al.*, 2002) which each have different absorption spectra. There has also been research into inorganic compounds for use in SAMs (Imahori *et al.*, 1999), (Bharathi, Nogami, & Ikeda, 2001). For an example; spectra of a porphyrin dye on a SAM see Figure 16 (Uosaki *et al.*, 1997): The dotted line represents the absorption spectra of a porphyrin in a SAM; the solid line represents the photocurrent that is generated as a function of wavelength. The inset diagram shows the difference in energy levels between the gold substrate, SAM, and electrolyte solution.

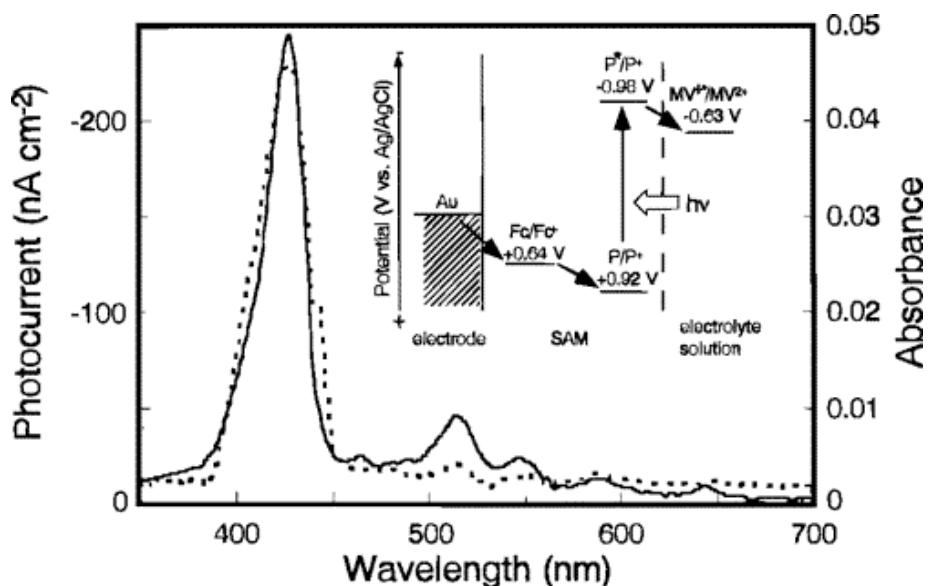


Figure 16 (Uosaki *et al.*, 1997): The dotted line represents the absorption spectra of a porphyrin in a SAM; the solid line represents the photocurrent that is generated as a function of wavelength. The inset diagram shows the difference in energy levels between the gold substrate, SAM, and electrolyte solution.

A thin film based cell works very similarly to a Grätzel cell with the use of an electrolyte and a cathode and an anode. The difference comes from the way the layer is constructed on the cathode. In a Grätzel cell the TiO_2 and a dye are used. In a thin film a linking molecule, which is typically either a carboxylic or sulfuric, that binds with the gold layer (Bharathi *et al.*, 2001), (Terasaki *et al.*, 2002), (Driscoll *et al.*, 2008). This can have another molecule attached onto the other end.

Part of the interest of multilayered thin films is the fact that different components can be placed in a particular order in order to achieve different interactions with the rest of the cell and prevent electrons from moving backwards along the chain of molecules (Uosaki *et al.*, 1997).

Driscoll *et al.* describe how the reduction potential of each component of an organic solar cell drives the photocurrent and photovoltage the cell produces (Driscoll, 2008). As shown in Figure 17 gold working electrode has a more negative reduction potential than the dye it is coated with, when the dye is in its ground state. The methyl viologen in the electrolyte also has a more negative reduction potential than the dye in its ground state, so provided the dye stays in its ground state no current or potential are generated.

When the dye, in this case a pyrene group (Py), is excited by a photon its reduction potential decreases from +1.2 V to -2.09 V making it more negative than methyl viologen. This drives the reduction of the methyl viologen by the porphyrin, injecting an electron into the electrolyte solution. The added charge causes a methyl viologen at the counter electrode to oxidize, passing current into the counter electrode. Since the dye again has a reduction potential below that of the gold after it is oxidized by the methyl viologen, an electron from the gold electrode will regenerate its ground state electron, thus completing the solar cell's electrical circuit and generating photocurrent.

The photovoltage of this system comes from the accumulation of conduction band electrons on the working electrode, which are limited in their ability to inject into the solution by the availability of methyl viologen which was not yet been reduced, which is dependent on the concentration of methyl viologen. This is very similar to the system used in this project, shown in Figure 18.

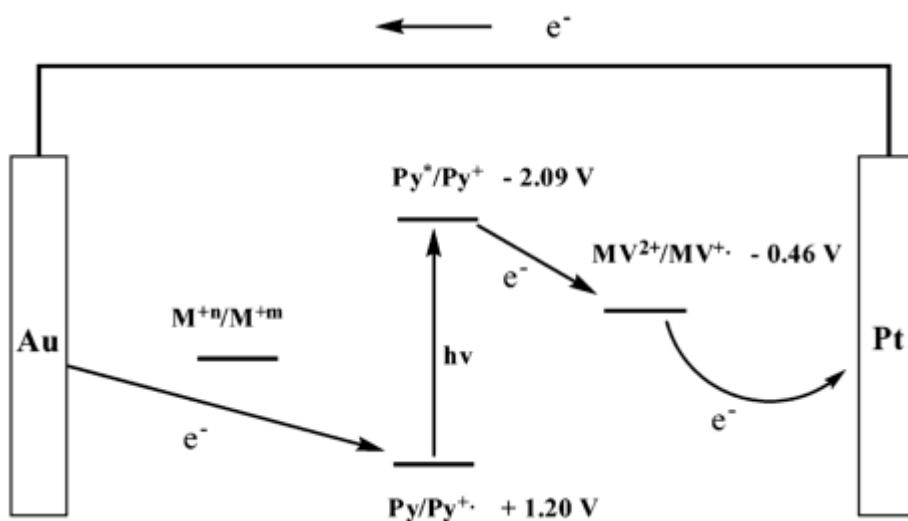


Figure 17 (Driscoll, 2008): Mechanism for generating photovoltage and photocurrent in the thin-film organic solar cell used by Driscoll *et al.*

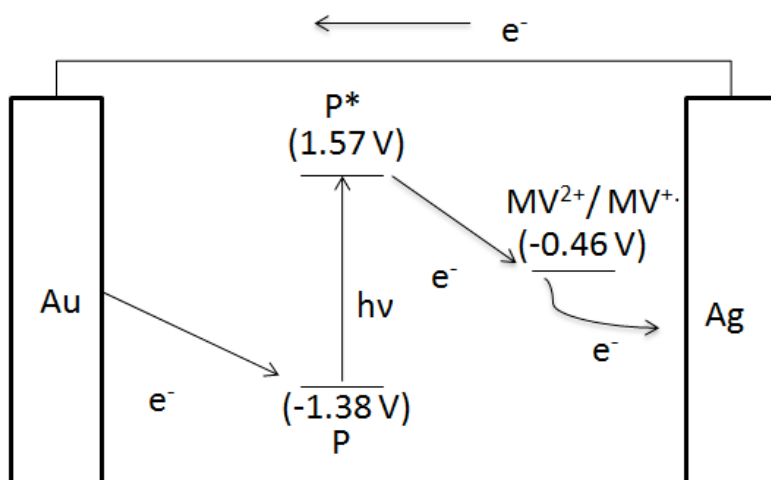


Figure 18: Mechanism for generating photovoltage and photocurrent in the thin-film organic solar cell used in this project.

2.6 Testing Procedures

When testing thin films and Grätzel cells a three-electrode set-up is traditionally used in order to measure the voltage and photocurrent (Bharathi *et al.*, 2001), (Fujihira *et al.*, 1985). In order to set this up typically the cell is submerged in a solution containing an electrolyte and then a platinum counter electrode and a silver reference electrode are placed in the solution with the sample.

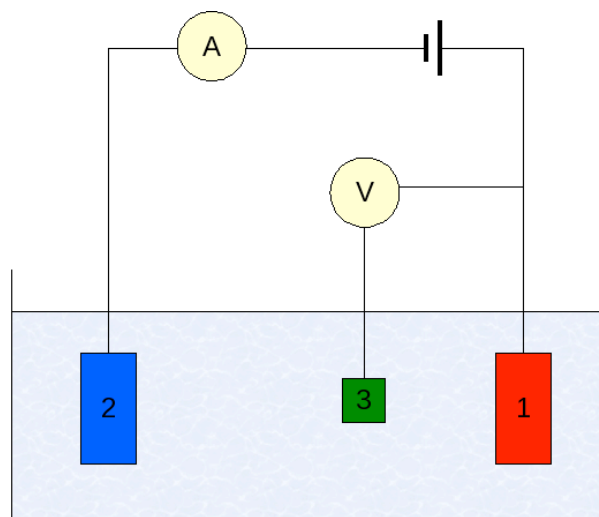


Figure 19 (Klimas, 2009): **1) The sample 2) The auxiliary electrode 3) The Reference Electrode. The Reference electrode stays at a constant voltage to allow for measurements of the voltage to be made and the auxiliary electrode provides current to make up for the flow of electrons through the solution.**

In the case of a Grätzel cell a similar set-up can be used. When this is done with a Grätzel cell the slide opposite to the slide with the TiO_2 is omitted (Campbell *et al.*, 2004; Wang *et al.*, 2009). It is also possible to leave a Grätzel cell completely constructed and a multimeter is used to test the current and voltage coming from the cell (Giannouli, Syrokostas, & Yianoulis, 2010).

2.7 Effects of Surface Topography on Efficiency

As mentioned in the overview of thin films and Grätzel cells there has been a good deal of research into increasing the incident photon to current efficiency (IPCE) of these technologies, which involves enhancing both the absorption of incident photons, and enhancement of the quantum yield. Towards this end we are measuring the effect the surface topography of the gold substrate of the SAM has on the IPCE. A variety of methods have been pursued for characterizing and changing the surface topography, as described in this section.

2.7.1 Electrical and Topographic AFM

Groves *et al.* (Groves, Reid, & Ginger, 2010) investigated the use of topographic and electrical AFM to characterize how the morphology of the surface of polymer organic solar cells affects the efficiency of the donor-acceptor heterojunction (Groves *et al.*, 2010). They demonstrated that this morphology has a high degree of heterogeneity. This heterogeneity makes the cell's structure vary based on the location scanned and as such it is difficult to determine the best possible way to improve the entire cell with one modification. With AFM they were able to measure the characteristics of the morphology on the nanoscale, with resolution between 10 and 100 nm. Figure 20 shows the AFM setup used for these measurements. Figure 21 shows the characterization. Significant heterogeneities were observed with variation of the photocurrent spanning an order of magnitude within a 1.5 micron scan. Sections spanning 20 to 100 nm had uniform photocurrent generation for the given incident light. This suggested distinct regions where the morphology caused high photocurrents, and regions in which it caused low photocurrent. Findings included that large domains favor geminate pair separation, while finer domains are needed to maximize exciton dissociation.

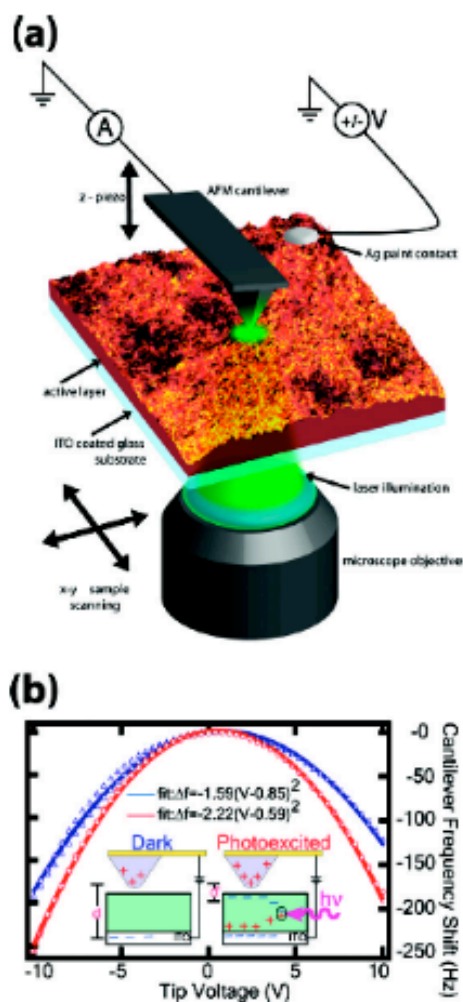


Figure 20 (Groves *et al.*, 2010): Schematic diagram of the pcAFM (trEFM) measurement system: a conducting AFM tip is co-aligned with a laser (or pulse LED) to provide simultaneous electrical bias and optical excitation to a specific simultaneous electrical bias and optical excitation to a specific area of the sample. (b) Cantilever shift frequency versus tip bias in a trEFM measurement for a PFB/F8BT blend film in the dark (blue triangles) and under illumination (red circles); insert shows schematically the difference in charge distribution for the two cases, which leads to the measured electrostatic force gradient.

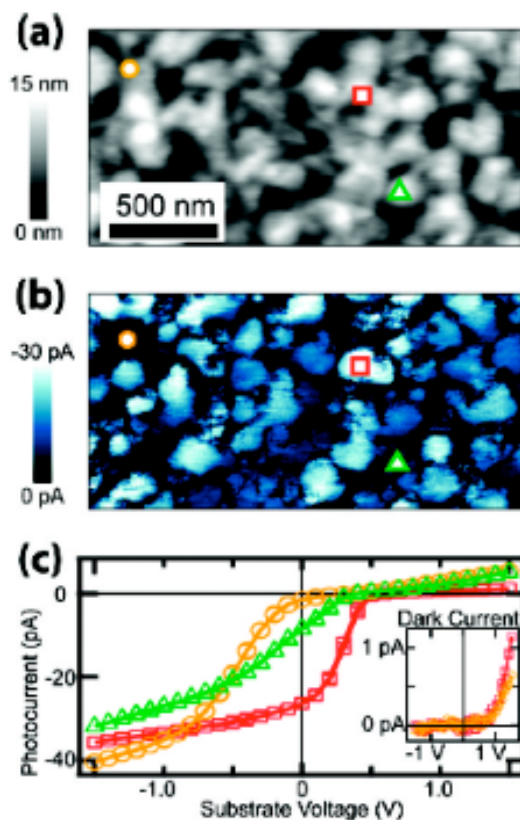


Figure 21 (Groves *et al.*, 2010): (a) AFM height image of an MDMO-PPV/PCBM (20:80 ratio) film spin-coated from xylene, (b) photocurrent map measured with zero external bias and an illumination intensity of 10^4 Wm^{-2} at 532 nm and (c) local current-voltage data acquired at the three locations indicated by the symbols in panels a and b. Insert shows local current-voltage data without illumination showing smaller dark currents.

Hoppe *et al.* (Hoppe *et al.*, 2004) also investigated the impact of surface morphology on the IPCE of organic solar cells. They characterized the bulk heterojunction of organic solar cells whose films are made of conjugated polymer/fullerene blends. By controlling certain parameters in the solution used to synthesize these cells, the authors were able to change the topography of the organic solar cell surface, as shown in Figure 22. Figure 23 shows the photoluminescence spectra of the surfaces characterized in Figure 22, among several other surfaces considered by Hoppe *et al.* in their publication. Photoluminescence is a sign of charge recombination, which results in the emission of absorbed light energy. This is a major contributor to inefficiency in organic solar cells, and suggests that the large height variation and feature size shown in Figure 22c will perform better than the small feature sizes of Figure 22a and Figure 22b. For the purposes of our project, this suggests that we may want to consider large feature size topographies for increasing the roughness of the gold substrate in our thin film organic solar cells.

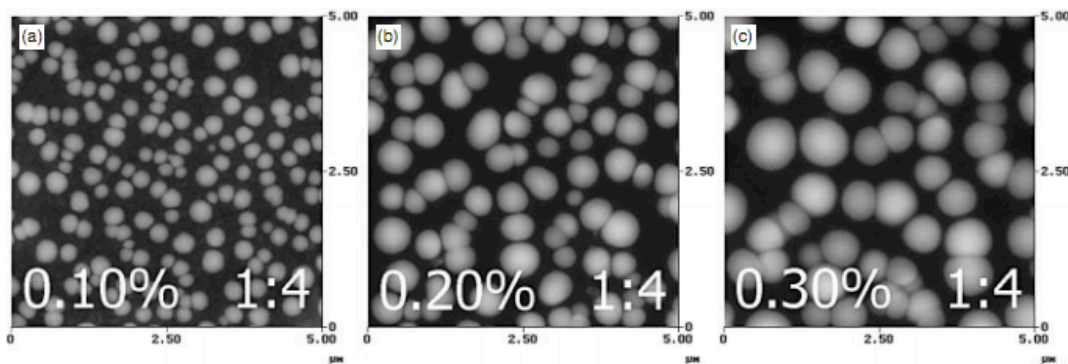


Figure 22 (Hoppe *et al.*, 2004): AFM scans of heterojunction photovoltaic films, each generated with a slightly different solution. The percent label corresponds to the concentration of part of the solution. Each solution generated a much different morphology of the heterojunction. Scan sizes are in all cases 5 μm x 5 μm; z-ranges are (a) 100 nm, (b) 150 nm, and (c) 200 nm.

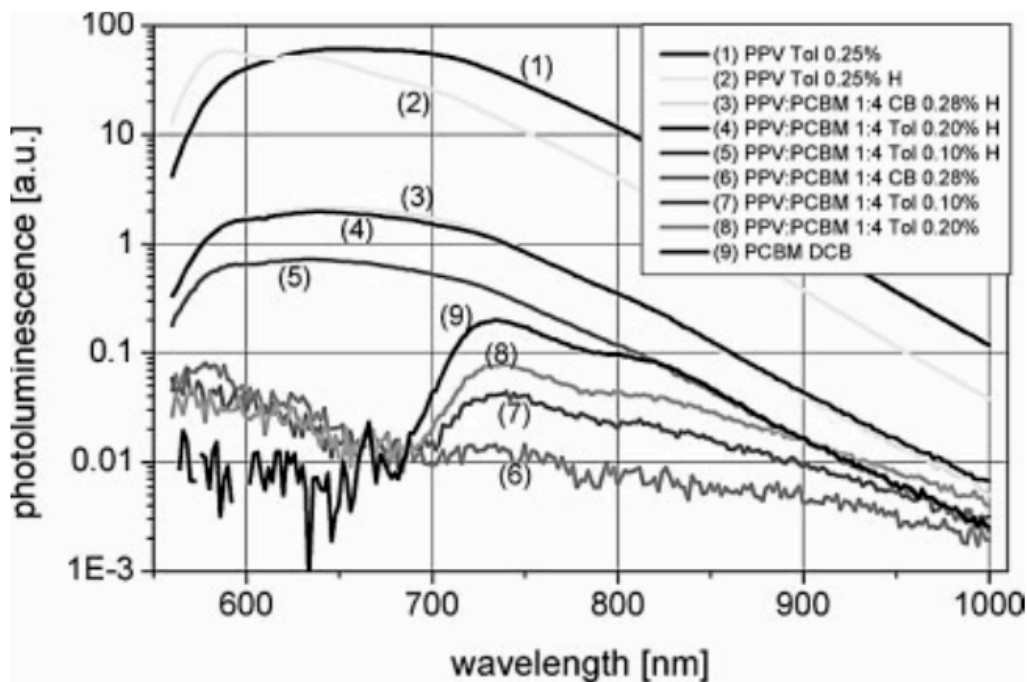


Figure 23 (Hoppe *et al.*, 2004): Photoluminescence spectra of films imaged in Figure 22, plus a number of other films. Films 3, 4, and 5 correspond to images c, b, and a in Figure 22. Caused by recombination of separated charges. This demonstrates that film 5 has greater quantum yield than 3 or 4.

2.7.2 Titanium Dioxide Nanotube Arrays

Tacconi *et al.* (de Tacconi, Chanmanee, Rajeshwar, Rochford, & Galoppini, 2009) grew titanium dioxide nanotube arrays (NTAs) of variable tube length and adsorbed monolayers of five different porphyrins (P1-P5) to photosensitize the surface. IPCE was measured as a function of wavelength for four different nanotube lengths with a monolayer of the porphyrin P3 (*Zn(II)-5,10,15,20-tetra (3-carboxyphenyl)*). The IPCE was also measured for each of the five porphyrins on two different nanotube lengths. The anchoring of P5 to the TiO₂ NTA is shown for reference in Figure 24, along with the molecular diagrams of all five porphyrins. Figure 25c shows the IPCE for each NTA tube length, the longest tubes providing the highest IPCE. This

suggests that a surface with greater roughness, and thus more porphyrins per unit area, will operate with a higher efficiency by absorbing more of the incident light.

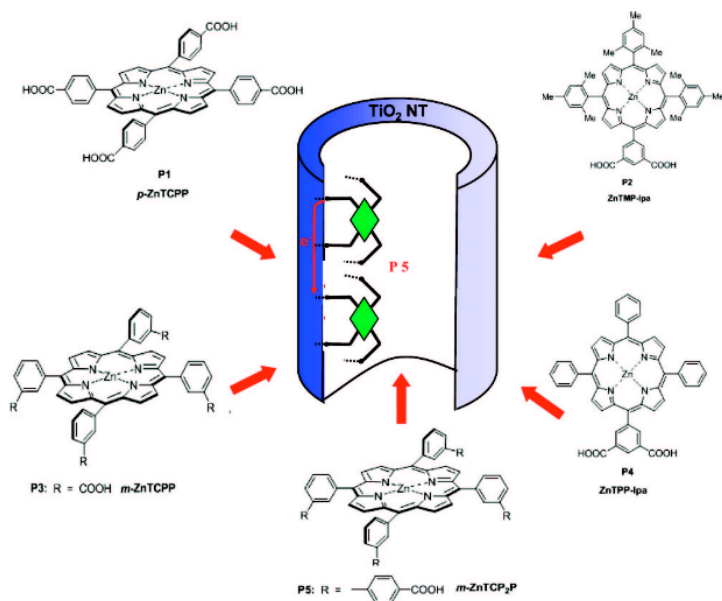


Figure 24 (de Tacconi *et al.*, 2009): Chemical structures of five porphyrin chromophores (P1-P5) used to sensitize TiO₂ NTAs. P5 is shown anchored to the inner wall of the TiO₂ nanotube.

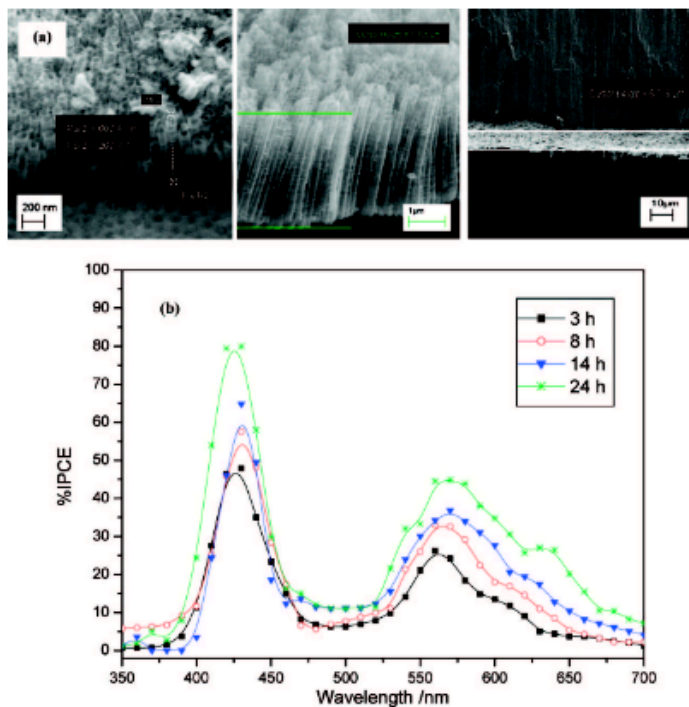


Figure 25 (de Tacconi *et al.*, 2009): **Results of the comparison Tacconi *et al.* did on the IPCE generated for NTAs of different height. (a) Cross-sectional SEM images of TiO₂ NTAs under the following anodic growth times: 3 h (left image), 8 h (middle), and 24 h (right). (b) Resultant photoaction spectra of these TiO₂ NTAs after sensitization with P3. The four IPCE-wavelength plots correspond to TiO₂ NTAs prepared with different anodization times (3, 8, 14, and 24 h).**

2.7.3 Donor Acceptor Heterojunction Morphology

Yang *et al.* (Yang, Shtein, & Forrest, 2005) controlled the surface morphology of the donor-acceptor (DA) heterojunction in the synthesis of certain organic photovoltaic cells. These cells consisted of molecular compounds that require high-evaporation temperatures. Two methods to deposit the molecules in a film on the active electrode were investigated, the organic vapor-phase deposition (OVPD) method and the more conventional vacuum thermal evaporation method (VTE), as they were found to produce different morphologies at the DA heterojunction. By properly controlling certain parameters in OVPD Yang *et al.* produced the morphology

Figure 25b. VTE produced the morphology in Figure 25a. Figure 26 shows a comparison of these two cell types, clearly demonstrating the supremacy of the morphology produced by OVPD for conversion incident light energy to electrical energy. The morphology produced by OVPD was also shown to perform much better than the flat junction shown in Figure 25a or the mixed junction shown in Figure 25d. While our solar cells are made of different materials from those generated by Yang *et al.*, their observations about which surface morphologies produce the highest conversion of light energy to electrical energy are valuable. They provide insight into what kind of surface topography would produce the highest photocurrent, open circuit voltage, and electrical power for a given incident illumination. For thin film solar cells the DA heterojunction is where the electrolyte contacts the photosensitive SAM, and for Grätzel cells where the electrolyte contacts the photosensitive film on the TiO₂ layer. Based on Yang *et al.*'s conclusions, our solar cells would perform best if the topography of the surface of our SAM or photosensitive film matched the one outlined in Figure 25b, since the same mechanisms of charger separation are at play at the heterojunction of our cells and those considered by Yang *et al.*

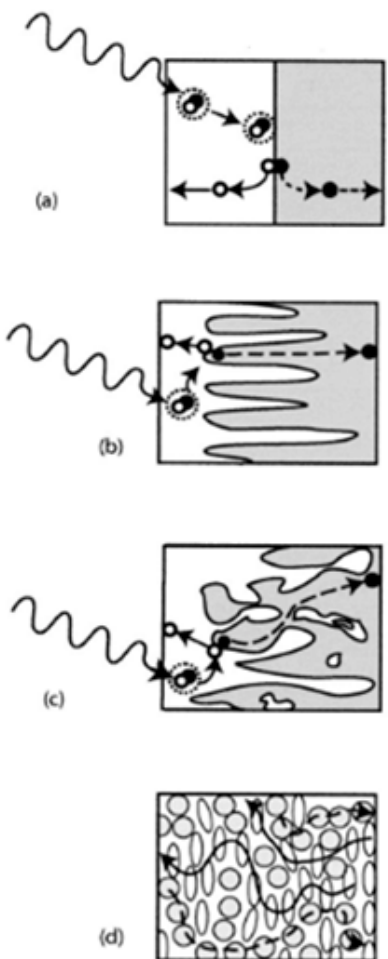


Figure 26 (Yang *et al.*, 2005): Schematic diagrams of the types of organic donor-acceptor (DA) heterojunctions used in organic photovoltaic cells. (a) Planar heterojunction. (b) Heterojunction with a large donor-acceptor interface area and continuous charge-carrier conducting pathways to the opposing electrodes formed by controlled growth with OVPD. (c) Heterojunction generated by VTE in which the carrier conducting pathways contain resistive bottlenecks and cu-de-sacs. (d) Mixed DA heterojunction in which the donor (white ellipsoids)-acceptor (gray circles) molecules create percolating pathways for conduction of charge carriers (arrows) that are generated by exciton dissociation at the contacts between the different molecules. Electrons (closed circles), holes (open circles), and excitons (circles enclosed by dashed line) are shown.

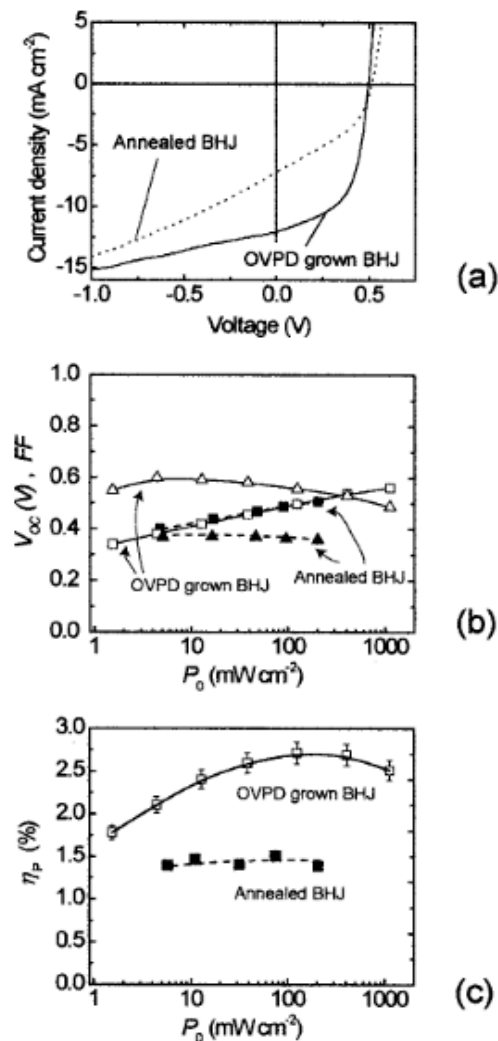


Figure 27 (Yang *et al.*, 2005): Performance characteristics of heterojunction photovoltaic devices grown by OVPD and by high-temperature annealing of VTE-grown mixed layers (a) Current density-voltage characteristics under 1 sun (100 mW/cm²), simulated air mass 1.5 global illumination, (b) open circuit voltage V_{OC} (squares), and fill factor FF (triangles), as functions of the illumination intensity, and (c) power conversion efficiency η_p , as a function of the illumination intensity for both devices. These graphs demonstrate that the heterojunction created with OVPD (morphology in Figure 25b) generates more photocurrent, open circuit voltage, and power for a given incident illumination than the cell created with VTE (morphology in Figure 25c).

2.7.4 Porphyrins on Gold Nano-Particles

Rather than use different NTA tube lengths to change the roughness of the substrate, we plan to deposit gold nano-particles onto a gold substrate. Hasobe *et al.* developed porphyrin (donor) and fullerene (acceptor) dye units by clusterization of gold nano-particles on SnO₂ electrodes as shown in Figure 28 below (Hasobe, Imahori, Kamat, & Fukuzumi, 2003). The scheme for developing these clusters is outlined in Figure 28. The focus of Hasobe *et al.* was to measure the incident photon to current efficiency (IPCE) of the nano-particle clusters on the SnO₂ for different concentrations of C₆₀ fullerene dye units. The greatest IPCE was found for the highest concentration of C₆₀, as shown in Figure 29. This study varies substantially from ours since we do not plan to change the dye used, but rather change the electrolyte and photosensitive material surface topography. Hasobe *et al.* made no comparison between the nano-clusters and any other surface for the dye arrangement he used. However, the nano-particle arrangement they derived offers a model for the development of a rough gold surface with nano-particles sensitized by porphyrin dyes. We can use this as one of several gold surface topographies for the study of the impact topography has on the IPCE of porphyrin sensitized organic solar cells. Other investigations of the use of gold nano-particles to generate unique porphyrin sensitized electrodes include Lu *et al.* who investigated the use of gold nano-particles sensitized with porphyrin molecules to create multilayer self assembled monolayers (SAMs) (Lu, Zhi, Shang, Wang, & Xue, 2010).

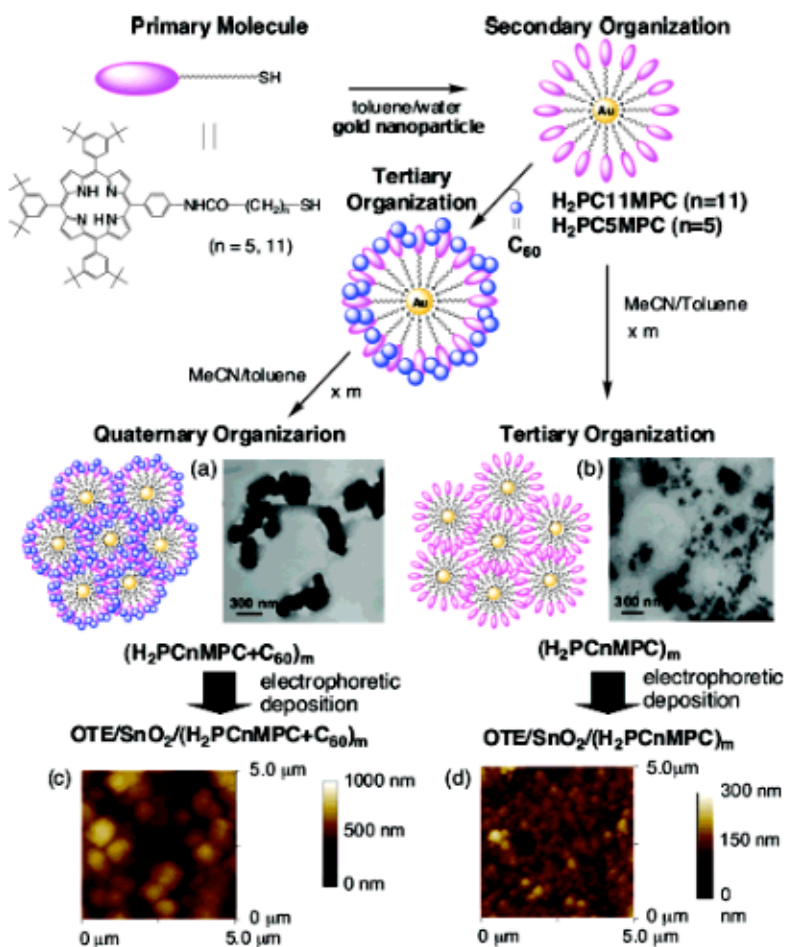


Figure 28 (Hasobe *et al.*, 2003): Structure of the high-order organization of porphyrin and C_{60} units with gold nano-particles and their TEM image of (a) porphyrin and C_{60} on nano-particle clusters ($\text{H}_2\text{PC11MPC} + \text{C}_{60}$), (b) only porphyrin on nano-particle clusters ($\text{H}_2\text{PC11MPC}$). AFM image of nano-particle clusters adhered to a gold substrate, sensitized with (c) porphyrin and C_{60} , (d) porphyrin.

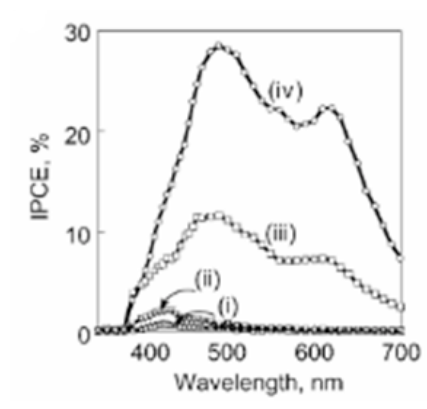


Figure 29 (Hasobe *et al.*, 2003): The photocurrent action spectra (IPCE vs. wavelength) of the gold nano-particle clusters on the SnO₂ substrate for different C₆₀ concentrations in the solution used to add the C₆₀ to the porphyrin coated nano-particles. The solutions had [H₂P] = 0.19 mM; [C₆₀] = (i) 0mM, (ii) 0.06 mM, (iii) 0.19 mM, and (iv) 0.31 mM in acetonitrile/toluene = 3/1.

2.7.5 Summary of the Effects of Surface Topography on Efficiency

Each of the above experiments addresses an aspect of this project. Groves *et al.* (Groves, Reid, & Ginger, 2010) used AFM to investigate the effects of nanoscale surface morphology on the efficiency of organic solar cells. Hoppe *et al.* (Hoppe *et al.*, 2004) made a similar investigation; he analyzed how the bulk efficiency of organic solar cells was impacted by the feature size of the topography, concluding that larger feature sizes had greater efficiency. Tacconi *et al.* (de Tacconi, Chanmanee, Rajeshwar, Rochford, & Galoppini, 2009) were chiefly concerned with the how different porphyrin molecules would arrange themselves on TiO₂ NTA, but included in their work an analysis of how NTA tube length affected efficiency. Here they demonstrated that longer tubes (and thus a rougher surface) provided a higher IPCE efficiency. This backs up our hypothesis that adding gold nano-particles to the gold substrate of our thin-film solar cell to increase the surface area will increase the efficiency of our cell. Yang *et al.* (Yang, Shtein, & Forrest, 2005) provide insight into what type of surface morphology provides

the best IPCE by investigating the process of electron and exciton transfer through different morphologies. This demonstrated the value of having both a high surface area at the cell's heterojunction, but also continuous charge conducting pathways devoid of resistive bottlenecks or cu-de-sacs. Hasobe *et al.* (Hasobe, Imahori, Kamat, & Fukuzumi, 2003) investigated the use of gold nano-particles as a base for the development of a porphyrin terminated SAM. This demonstrates that the surface roughened with gold nano-particles, we plan to compare to a flat surface, should efficiently generate photocurrent.

References

- Barber, J., & Archer, M. D. (2001). P680, the primary electron donor of photosystem II. *Journal of Photochemistry and Photobiology A: Chemistry*, *142*(2-3), 97-106. doi:DOI: 10.1016/S1010-6030(01)00503-2
- Bharathi, S., Nogami, M., & Ikeda, S. (2001). Layer by layer self-assembly of thin films of metal hexacyanoferrate multilayers. *Langmuir*, *17*(24), 7468-7471. doi:10.1021/la011053c
- Bisquert, J., Cahen, D., Hodes, G., RÅ¼hle, S., & Zaban, A. (2004). Physical chemical principles of photovoltaic conversion with nanoparticulate, mesoporous dye-sensitized solar cells. *The Journal of Physical Chemistry B*, *108*(24), 8106-8118. doi:10.1021/jp0359283

- Campbell, W. M., Burrell, A. K., Officer, D. L., & Jolley, K. W. (2004). Porphyrins as light harvesters in the dye-sensitized TiO₂ solar cell. *Coordination Chemistry Reviews*, 248(13-14), 1363-1379. doi:DOI: 10.1016/j.ccr.2004.01.007
- Chen, C., Pootrakulchote, N., Wu, S., Wang, M., Li, J., Tsai, J., *et al.* (2009). New ruthenium sensitizer with carbazole antennas for efficient and stable thin-film dye-sensitized solar cells. *The Journal of Physical Chemistry C*, 113(48), 20752-20757.
doi:10.1021/jp9089084
- de Tacconi, N. R., Chanmanee, W., Rajeshwar, K., Rochford, J., & Galoppini, E. (2009). Photoelectrochemical behavior of polychelate porphyrin chromophores and titanium dioxide nanotube arrays for dye-sensitized solar cells. *The Journal of Physical Chemistry C*, 113(7), 2996-3006. doi:10.1021/jp808137s
- Driscoll, P. F., Douglass Jr, E. F., Phewluangdee, M., Soto, E. R., Cooper, C. G. F., MacDonald, J. C., *et al.* (2008). Photocurrent generation in noncovalently assembled multilayered thin films. *Langmuir*, 24(9), 5140-5145.
- Feldt, S. M., Gibson, E. A., Gabrielsson, E., Sun, L., Boschloo, G., & Hagfeldt, A. (2010). Design of organic dyes and cobalt polypyridine redox mediators for high-efficiency dye-sensitized solar cells. *Journal of the American Chemical Society*, 132(46), 16714-16724.
doi:10.1021/ja1088869
- Fujihira, M., Nishiyama, K., & Yamada, H. (1985). Photoelectrochemical responses of optically transparent electrodes modified with langmuir-blodgett films consisting of surfactant derivatives of electron donor, acceptor and sensitizer molecules. *Thin Solid Films*, 132(1-

4), 77-82. Retrieved from <http://www.sciencedirect.com/science/article/B6TW0-46YKSYD-N8/2/a288a19879d363e3127d7c6caafc9be9>

Giannouli, M., Syrokostas, G., & Yianoulis, P. (2010). Effects of using multi-component electrolytes on the stability and properties of solar cells sensitized with simple organic dyes. *Progress in Photovoltaics*, 18(2), 128-136. doi:10.1002/pip.952

Govindjee, & Coleman, W. J. (1990). **How plants make oxygen**. *Scientific American Adf*, 262(2), 50-50-5, 58.

Grätzel, M. (2003). Dye-sensitized solar cells. *Journal of Photochemistry and Photobiology*, , 145.

Groves, C., Reid, O. G., & Ginger, D. S. (2010). Heterogeneity in polymer solar cells: Local morphology and performance in organic photovoltaics studied with scanning probe microscopy. *Accounts of Chemical Research*, 43(5), 612-620. doi:10.1021/ar900231q

Grunwald, R., & Tributsch, H. (1997). Mechanisms of instability in ru-based dye sensitization solar cells. *The Journal of Physical Chemistry B*, 101(14), 2564-2575. doi:10.1021/jp9624919

Hasobe, T., Imahori, H., Kamat, P. V., & Fukuzumi, S. (2003). Quaternary self-organization of porphyrin and fullerene units by clusterization with gold nanoparticles on SnO₂ electrodes for organic solar cells. *Journal of the American Chemical Society*, 125(49), 14962-14963. doi:10.1021/ja0377192

- Hoppe, H., Niggemann, M., Winder, C., Kraut Jurgen, Hiesgen, R., Hinsh, A., *et al.* (2004). Nanoscale morphology of conjugated Polymer/Fullerene-based bulk-heterojunction solar cells. *Advanced Functional Materials*, 14(10), 1005-1005-1011.
- Imahori, H., Azuma, T., Ajavakom, A., Norieda, H., Yamada, H., & Sakata, Y. (1999). An investigation of photocurrent generation by gold electrodes modified with self-assembled monolayers of C60. *The Journal of Physical Chemistry B*, 103(34), 7233-7237.
doi:10.1021/jp990837k
- Klimas, S. J. (2009). *Three electrode setup*
http://upload.wikimedia.org/wikipedia/commons/2/2f/Three_electrode_setup.png
- Lu, X., Zhi, F., Shang, H., Wang, X., & Xue, Z. (2010). Investigation of the electrochemical behavior of multilayers film assembled porphyrin/gold nanoparticles on gold electrode. *Electrochimica Acta*, 55(11), 3634-3642. doi:DOI: 10.1016/j.electacta.2009.11.004
- Prahl, S.
Tetraphenylporphyrin (TPP). Retrieved 12/17, 2011, from
<http://omlc.ogi.edu/spectra/PhotochemCAD/html/TPP.html>
- Pullerits, T., & Sundstrom, V. (1996). Photosynthetic light-harvesting pigment-protein complexes: Toward understanding how and why. *Department of Chemical Physics*, 29, 381-381-389.

- Scheuring, S. (2006). AFM studies of the supramolecular assembly of bacterial photosynthetic core-complexes. *Current Opinion in Chemical Biology*, 10(5), 387-393. doi:DOI: 10.1016/j.cbpa.2006.08.007
- Scheuring, S., & Sturgis, J. N. (2009). *Atomic force microscopy of the bacterial photosynthetic apparatus: Plain pictures of an elaborate machinery.(report)* Retrieved from http://find.galegroup.com/gtx/infomark.do?&contentSet=IAC- Documents&type=retrieve&tabID=T001&prodId=AONE&docId=A232211906&source=gale&srcprod=AONE&userGroupName=mclin_c_worpoly&version=1.0
- Sharma, C. V. K., Broker, G. A., Szulczewski, G. J., & Rogers, R. D. (2000a). Self-assembly of freebase- and metallated-tetrapyridylporphyrins to modified gold surfaces. *Chemical Communications*, (12), 1023-1024. Retrieved from <http://dx.doi.org/10.1039/B002084M>
- Sharma, C. V. K., Broker, G. A., Szulczewski, G. J., & Rogers, R. D. (2000b). Self-assembly of freebase- and metallated-tetrapyridylporphyrins to modified gold surfaces. *Chem. Commun.*, (12), 1023-1024. doi:10.1039/B002084M"
- Terasaki, N., Akiyama, T., & Yamada, S. (2002). Structural characterization and photoelectrochemical properties of the self-assembled monolayers of tris(2,2'-bipyridine)ruthenium(II)⁺Viologen linked compounds formed on the gold surface. *Langmuir*, 18(22), 8666-8671. doi:10.1021/la025936v
- Uosaki, K., Kondo, T., Zhang, X., & Yanagida, M. (1997). Very efficient visible-light-induced uphill electron transfer at a self-assembled monolayer with a

- PorphyrinâFerroceneâThiol linked molecule. *Journal of the American Chemical Society*, 119(35), 8367-8368. doi:10.1021/ja970945p
- Veronica Szalai, G. B. (1998). How plants produce dioxygen. *American Scientist*, 86(6), 542-543-552.
- Wang, Z., Koumura, N., Cui, Y., Miyashita, M., Mori, S., & Hara, K. (2009). Exploitation of ionic liquid electrolyte for dye-sensitized solar cells by molecular modification of organic-dye sensitizers. *Chemistry of Materials*, 21(13), 2810-2816. doi:10.1021/cm900544j
- Yang, F., Shtein, M., & Forrest, S. R. (2005). Morphology control and material mixing by high-temperature organic vapor-phase deposition and its application to thin-film solar cells. *Journal of Applied Physics*, 98(1), 014906-014906-10.
- Zhao, Y., Zhai, J., He, J., Chen, X., Chen, L., Zhang, L., *et al.* (2008). High-performance all-solid-state dye-sensitized solar cells utilizing imidazolium-type ionic crystal as charge transfer layer. *Chemistry of Materials*, 20(19), 6022-6028. doi:10.1021/cm800673x

Chapter 3. Methods Chapter

3.1 Introduction

In this chapter the methods and technologies used for the construction and measurement of the samples will be explained. The unsuccessful as well as the successful and final set-ups will be given an overview. Fabrication of the cells went through much iteration and used many different types of equipment. There were several “arts” that needed to be learned while constructing the cells in order to produce consistent results. Challenges are outlined for the development of a viable testing set-up that would offer consistent results with a low signal to noise ratio. The testing of the cells ultimately yielded promising results. Several recommendations are included for any party interesting in continuing this work.

3.2 Grätzel Cell

3.2.1 Construction

To construct an organic solar cell a dye molecule must be attached to a substrate. In the case of the Grätzel cell this is accomplished through a layer of titanium dioxide that attaches the dye molecule to a metal substrate.

Grätzel cell construction starts by taking a metal-coated slide, in our case a gold slide, and cutting it in half. The slide is then cleaned in an ethanol bath in a sonicator for 20 minutes and dried using nitrogen (Grätzel, 2003).

Next a 10 ml mixture of 1% acetic acid and de-ionized water is mixed with 6 grams of titanium dioxide with a mortar and pestle to form a smooth paste. It was found that too much

mixing of this causes bubbles to be introduced into the mixture, which causes inconsistencies in the final product.



Figure 30: Mixture of titanium dioxide and 1% acetic acid solution.

After the mixture of titanium dioxide is created, the half slides are taped down, metal side up, along three of the four edges with scotch tape. A small drop of the titanium dioxide is placed near the edge opposite the edge that was not taped and a glass stir rod is used to carefully spread the droplet downward, allowing it to cover the entire untapped surface of the slide. The most consistent results were obtained when the stir rod was not rolled while spreading the titanium dioxide, this produced the least amount of streaking and most uniform surface. Only apply gentle pressure downward while spreading; this will yield the most uniform thickness of the titanium dioxide layer.

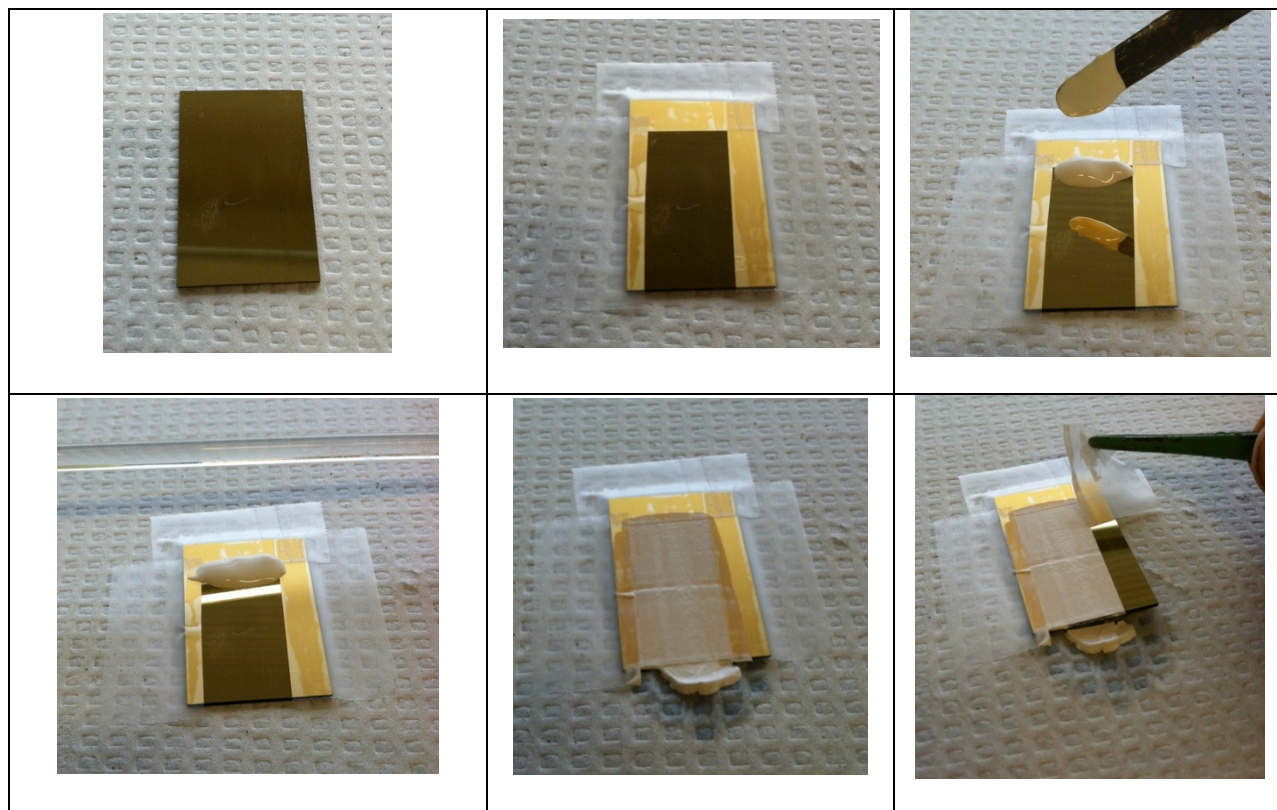


Figure 31: Steps for depositing titanium dioxide layer on gold slide

Once this has been finished the slides are placed on a hot plate, which is then placed at maximum heat ($>500\text{ C}$) after the slides are placed on it. The slides are left for approximately 30 minutes where they will turn a greenish / yellowish hue until heat is removed; this is the sintering process, which allows the titanium dioxide to dry, and it allows the powder to reform into a crystalline structure that adheres to the surface of the slide.



Figure 32: Grätzel Cell on hot plate, prepared to be sintered

During the heating process a 2 mM porphyrin solution in tetrahydrofuran (THF) is prepared. After experimenting with different solvents it was found that THF was the solvent that provided the best absorption of the porphyrin onto the titanium dioxide layer.

Dimethylformaldehyde (DMF) can also be used as a solvent. The porphyrins used in our experiments were initially tetrapyrrolyl porphyrin and tetraphenyl porphyrin. Tetrapyrrolyl porphyrin was used most extensively because it possesses a pyridyl group that will hydrogen bond to other materials.

Once the porphyrin solution is finished and the titanium dioxide coated slides have been on the hot plate for 30 minutes, the hot plate should be shut off. When the temperature of the cells is between 50 and 80 degrees Celsius the cells are then removed and placed in a crystallization dish with enough porphyrin solution to cover them. Parafilm is then stretched over the surface of the dish and the dish placed in a completely dark location for a minimum of 12 hours, the parafilm will not be dissolved by the THF.



Figure 33: Grätzel Cell in porphyrin solution.

During this time a set of transparent metal-coated slides, in this case Indium Tin-Oxide (ITO) is prepared for the other side of the cell. First the slides are cut to size so that they are roughly the same length as the titanium dioxide coated slides. Next an ohmmeter should be used to determine which side of the slide is coated with ITO, and a scratch should be made in the top left corner of the non-coated side of each half slide to mark this. The slides should then be cleaned with a 20 minute bath in ethanolamine.

Before final construction of the cell a mixture of 2 mM iodine and 20 mM potassium iodide should be mixed in de-ionized water; this will act as the electrolyte solution in the cell. The ITO slides should be plasma cleaned and the titanium dioxide coated slides should be carefully removed from their dish and rinsed with THF and blown dry with nitrogen. The slides should then be placed together with the titanium dioxide layer of the first slide and the ITO coated side of the second slide touching. Make sure to leave a 2-3 mm tab on either side of the cell, each exposing one of the metal-coated sides for electrical connection *via* alligator clips. A small droplet of the electrolyte solution should then be touched to the slide of the cell so that capillary action will draw it into cell.

Finally the cells should be wrapped in parafilm to prevent electrolyte leakage. Silicone was also experimented with as a sealant, but gave less consistent results than the parafilm. The sealant should be prevented from covering the ITO slide so that light can reach the titanium dioxide layer unhindered. Likewise the 2-3 mm tabs on either end of the cell should not be completely covered with sealant so that they can still be contacted with alligator clips. This was accomplished by covering the cells entirely with parafilm and using a scalpel to cut a window on the ITO slide for light and windows on the tabs for electrical contact.

3.2.2 Difficulties

One of the primary difficulties was producing cells consistently with minimal streaking of the titanium dioxide layer and with uniform dye absorption. Careful experimentation and repeated attempts made the cells more consistent over time.

The electrolyte can also prove to be a challenge. Because of its relatively volatile nature it evaporates very quickly and is not easy to seal. As noted above, parafilm was found to be the most effective way to seal the cells.

One method that was debated for future use was submerging the cells in a bath of the electrolyte until use. This prevented the problems associated with drying out the cells and having to recharge them, which could change the concentration of the electrolyte. This method ultimately did not cause the cells to revive.

Measurements of photocurrent and photovoltage were most consistently made with an oscilloscope and multimeter. The high impedance setting on the oscilloscope must be used to measure the low current and voltage produced by the cell, rather than the low impedance setting. Measurements with a potentiostat and a three-electrode set-up proved very challenging, despite the advantage of forwarding and reverse biasing the cell that this arrangement offered.

When using a three electrode set-up with the Grätzel cells, the ITO slide and parafilm covering was removed from the construction, and the gold slide was used as the working electrode submerged in a bath of the electrolyte solution. The biggest challenge with this set-up was that the bias introduced by the three-electrode set-up was capable of very quickly dissolving the gold from the Grätzel cell, rendering it useless. Attempting to set the bias to zero also produced stripping of the gold from the glass and helped us come to the conclusion that the potentiostat was defective. There were also problems with the acidity of the electrolyte solution, which very quickly dissolved the titanium dioxide layer. Eventually the testing of the Grätzel cells in the three-electrode set-up was dropped due to these difficulties. For future experiments, the use of a three electrode set-up with Grätzel cells is not recommended; a simple multimeter, oscilloscope, or lock-in amplifier set-up is recommended to measure photocurrent and photovoltage.

3.3 Thin-Film Solar Cell

3.3.1 Thin-Film Solar Cell Construction

Thin-film solar cells are composed of a self assembled monolayer (SAM), the construction of which occurs in multiple stages. First the substrate (in this case a gold slide) was cut into 1 cm by 2 cm pieces. It is helpful to score a line across the back of the pieces 1 cm from the bottom so that when the cells are finished and placed in solution exactly 1 cm of square surface area can be easily submerged for consistent testing purposes. In order to clean the slides the pieces of the slide were bathed in a nitric acid solution for 5 minutes, and were rinsed off and dried using nitrogen.

In order to attach the first linking molecule to the surface of the cleaned gold slides, the slides were immersed in a Mercaptoundecanoic acid (MUA) solution of ethanol and allowed to

sit overnight. This attaches the MUA layer to the gold by causing the acid on the end of the MUA molecule to adhere to the gold surface.

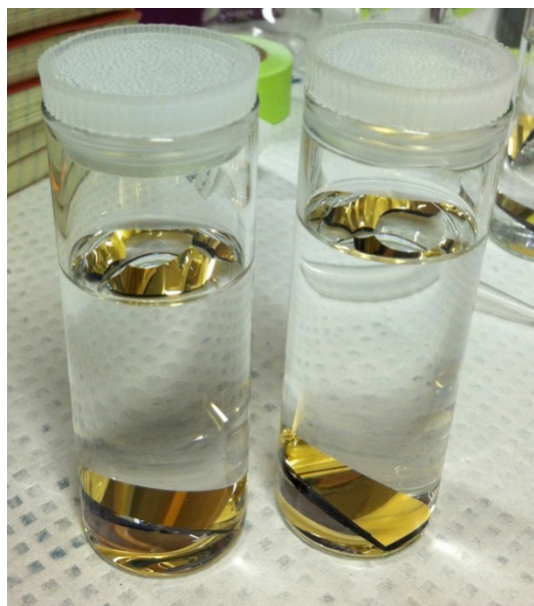


Figure 34: Gold slides in MUA solution

After the slides have been allowed to sit in this bath overnight they are removed, rinsed with ethanol, dried with nitrogen, and surface angle measurements to confirm the attachment of the MUA molecules. By this stage the slides are ready to have a dye molecule attached.



Figure 35: Gold slides in porphyrin solution, post MUA solution

In this experiment tetrapyrrolyl porphyrin was attached to the surface by bathing the cells in a porphyrin and chloroform solution for a minimum of 12 hours. A sample cell was removed from the solution, rinsed with ethanol, dried with nitrogen, and characterized with UV-Vis spectrum analysis to confirm that the porphyrin was attached to the surface. The cells were then kept in the dark, in solution, until needed for testing. When the batch of cells was ready for testing, they were removed, rinsed with ethanol and dried with nitrogen. In this experiment the cells were stored dry for durations of time from between 1 day and one month depending upon the batch. (Driscoll *et al.*, 2008). While Driscoll's cell's are different from the ones produced in this experiment, it was found that the cells did remain viable after a period of 3-4 weeks sitting in the solution.

3.3.2 Difficulties

Issue arose with taking the cells out of the porphyrin solution and rinsing them with ethanol. The chloroform that the porphyrin is dissolved in evaporates very quickly, and will often evaporate and leave a deposit of crystalline porphyrin before it can be rinsed off with ethanol.

This produces cells very inconsistently. To remedy this problem, each cell is taken out of the phial with the porphyrin and chloroform solution and put into a Petri dish with the same solution. This makes it easier to take the slide out the solution so that the chloroform can be rinsed off the slide with ethanol within a second, before it evaporates. The slide should look clear without any stain or visible residue.

3.4 Rough Surface Construction

Rough surfaces are prepared by first being cut and cleaned in the same method as when constructing a SAM. The slides are then deposited in a solution of dithiol linking molecules and cleaned in a solution. This allows for the attachment sites of the gold seeds that will grow into the nano-particles.



Figure 36: Gold slides in cleaning solution post dithiol attachment

After 30 minutes in this bath the slides are removed, rinsed with DI water and placed in the gold seed bath for 20 minutes. For larger nano particles, the slide can be left in this solution for a longer duration of time. The slides may be characterized by UV-Vis and surface angle

measurements prior to the gold seed bath to ensure that the linking molecules were successfully attached.

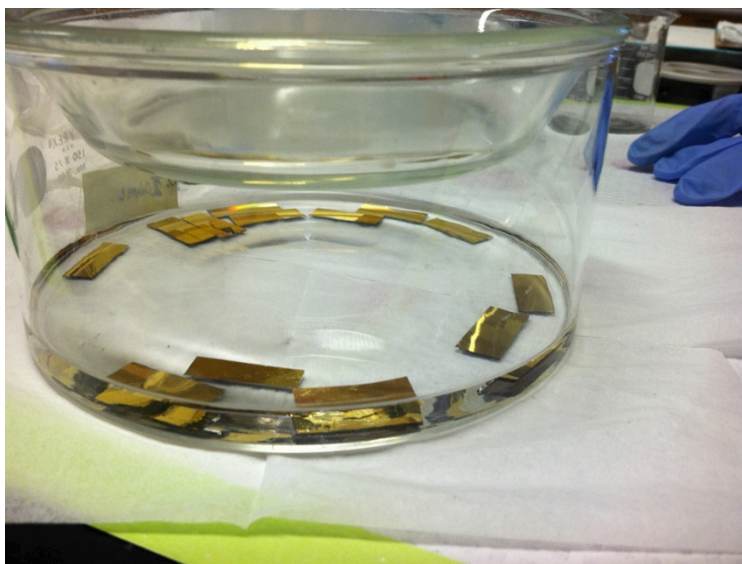


Figure 37: Gold slides in gold nanoparticle growth solution

After the slides have been removed from the gold seed bath they are placed in a growth solution of gold chloride for between 1 and 21 hours depending upon desired size of the nanoparticles. After this, the slides are removed from the solution, rinsed with DI water, and characterized by UV-Vis spectra analysis, contact angle measurements and AFM in order to determine surface topography. It should be noted that proper preparation of the solutions will yield clear solutions even for both the gold seed and growth solutions. This is because the growth of the gold does not occur in the solution but occurs directly on the surface of the slides. If growth is occurring in the solution (an undesired result) the growth solution can turn pink (Wei, Mieszawska, & Zamborini, 2004).

The same steps previously described in section 3.3 on SAM construction can then be used to produce a SAM on the rough surface.

3.5 Photoelectrochemistry Set-up

3.5.1 Final Set-up

The photoelectrochemistry set-up was used to irradiate the organic solar cells studied in this paper and measures the consequent photovoltage they produced. A schematic of the apparatus is shown in Figure 38.

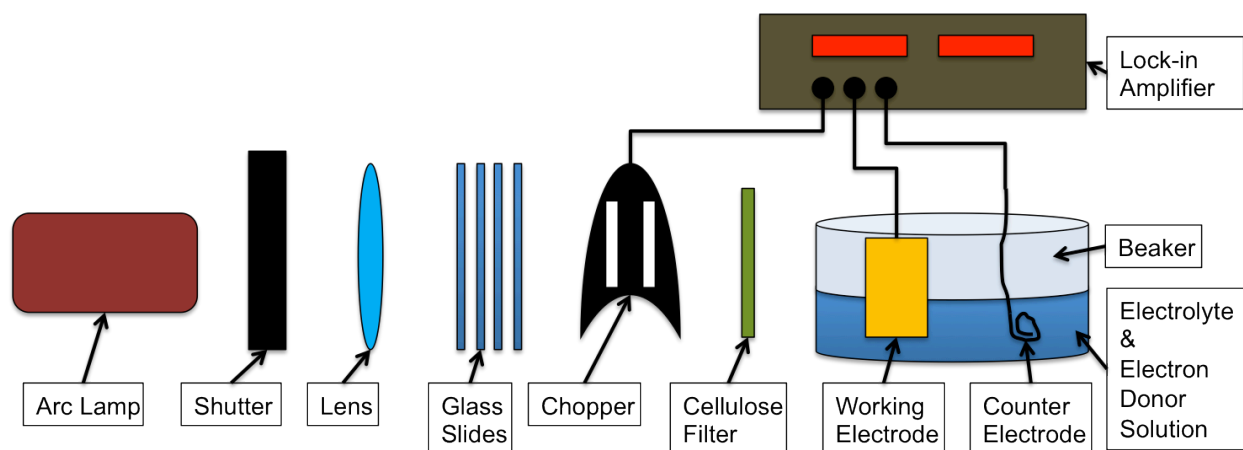


Figure 38: Schematic of photoelectrochemistry set-up used to measure photovoltage and photocurrent with a lock-in amplifier. The arc lamp provides irradiation and the shutter controls exposure of the sample to the irradiation. The lens is convex, made of quartz, and used to collimate the light beam from the lamp. The glass slides reduce the intensity of the irradiation, as each slide only transmits 94% of the incident radiation. The chopper cuts the light at a set frequency so the lock-in amplifier can filter out all other signals. The working electrode is the sample under investigation, and the counter electrode a silver wire coated with silver chloride. These are in solution to facilitate electron transfer between them.

Full spectrum irradiation was provided with a Xenon arc lamp operating at 70 watts. The lamp was always turned on at least 20 minutes before measurements were taken so that it could warm up; the power supply for the lamp generated significant line noise in measurement instrumentation when initially turned on. The lamp's focal point was 20 cm from the front of the lamp. A convex lens was placed 39 cm from the lamp to collimate the light beam; the lamps

focal point was at 26 cm. A cellulose filter made of tissue paper was used to diffuse the shadow cast by the electrode of the arc lamp. A mechanical shutter was used to control exposure of the sample so that the lamp could be kept on throughout the experiment. A horizontal stack of glass slides on a custom stand made out of a slide container was used to control the intensity of the light on the sample. The stand could hold up to 63 slides, each of which transmitted 94% of the incident light, allowing a maximum reduction of 10%. To determine the transmission of the stack of slides, stacks of 1 to stacks of 42 slides were measured with a UV Vis spectrometer. An exponential curve was fit to the data to extrapolate out to 63 slides; approximately the number of slides necessary to provide a reduction to 10% intensity. Figure 39 shows the experimental data, the curve fit to it, and the extrapolation point at 63 slides.

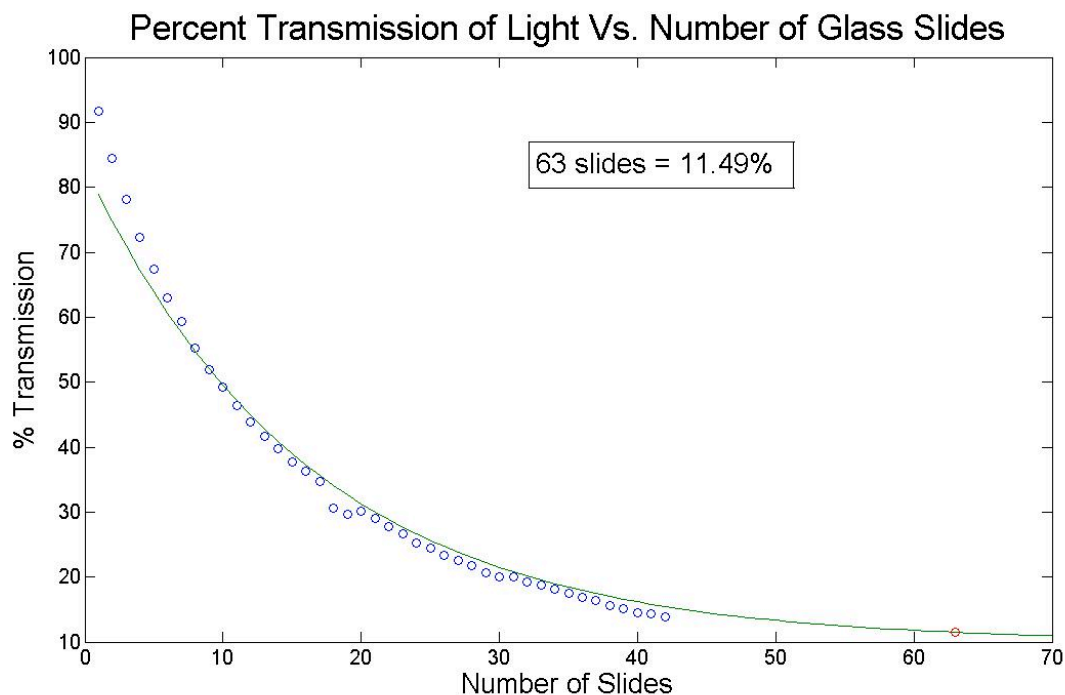


Figure 39: UV Vis measurements were made of the transmission of light through glass slides, to determine how many glass slides were necessary to sufficiently reduce the intensity of the irradiation from the arc lamp. An exponential curve was fit to the data to extrapolate out to 63 slides, the number of slides used in the setup to reduce the intensity by approximately 10%.

Filters were held in the light beam by a stand for spectroscopy experiments. As a safety precaution, a three-sided wooden box was used to cover the optics and block harmful UV radiation generated by the lamp. The working electrode was the solar cell under investigation, and the counter electrode a silver wire coated with silver chloride. Soaking the wire in bleach overnight generated the silver chloride layer. The silver chloride coating was deposited to provide a more stable potential between the wire and the solution. The solution was aqueous and composed of 1 mM methyl viologen as an oxidizing agent and 50 mM potassium chloride as a supporting electrolyte. All solutions were made fresh. Initially repeat use of solutions was avoided due to concerns about degradation of the methyl viologen. The working electrode was

contacted with an alligator clamp and 1 cm^2 was immersed in solution. Originally solutions were bubbled with nitrogen for 20 minutes in order to remove oxygen from the solution, but this practice was stopped so that the oxygen in the solution could regenerate the methyl viologen after it was reduced by the porphyrin.

Photovoltage measurements were taken with a Stanford Research Systems Model SRB 10 DSP lock-in amplifier. A two-electrode set-up was used where the first electrode was the sample cell and the second was another silver wire that had been dipped in concentrated HCl overnight. The noise level was low enough with the lock-in amplifier that the Faraday cage was not necessary. One important noise reduction technique to note though is the wiring of the electrodes. The wires should be twisted in order to prevent them from acting as a radio antenna and generating signal noise in the readings. With a lock-in amplifier the device must be set to the phase of the signal it is receiving. This is not necessarily the frequency of the chopper, as capacitive or inductive effects could create a phase shift. To acquire this the “auto-phase” feature of the instrument was used. To confirm that the phase was correct, the amplifier was periodically put 90 degrees out of phase to confirm that this gave a reading of zero. The readings that were obtained demonstrated that the device was properly finding the phase of both the PV and PI (“auto-phase” was used between every measurement of PV and PI in case there was a change between them). Table 1 shows some sample measurements.

Tests with Filters and Phasing						
<i>Cell</i>	<i>PV (μV)</i>	<i>PI (nA)</i>		<i>Cell</i>	<i>PV (μV)</i>	<i>PI (nA)</i>
NS1	0.252	0.218		NR1	0.23	0.355
+90 degrees out of phase	-0.102	0.064		+90 degrees out of phase	0.006	-0.031

Table 1: Measurements the PV and PI of a smooth and a rough solar cell with different phasing on the lock-in amplifier.

3.5.2 Set-up Problems Encountered & Trouble Shooting

This set-up went through several iterations to address a variety of issues encountered. A preliminary set-up used an oscilloscope to measure the PV of the solar cell. PI was also measured using Ohm's Law to convert to current the voltage across a 10 k Ω resistor in series with the solar cell and the counter electrode. This system was limited in its resolution and lacked the ability to impose a bias on the system.

A three electrode set-up (see section 3.5.3 below) with a potentiostat addressed these issues. A platinum wire was used for the counter electrode and a standard calomel electrode (SCE) for a reference electrode. The working electrode was the solar cell under investigation. Measurements were taken with an EG&G Princeton Applied Research Potentiostat/Galvanostat Model 273. The solution was aqueous and composed of 1 mM methyl viologen as a redox agent and 50 mM sodium sulfate as a supporting electrolyte. A Faraday cage was used to reduce noise. It was covered completely to reduce ambient light; a small slit in the cover allowed irradiation of the sample. This potentiostat set-up was modeled after the set-up used by Driscoll *et al.* (Driscoll *et al.*, 2008)

Chronoamperometry and cyclic voltammetry were used to determine the optimum bias voltage and the bleaching rate for the system. With this set-up the gold would separate from the glass slide when too large of a bias voltage was applied to the system. The resolution of the instrument was also insufficient to measure photocurrent at a zero bias voltage. Ultimately this set-up produced too much noise and it is believed that the potentiostat was defective and was over-volting the samples, causing the gold on the surface of the slides to dissolve. This was mitigated with the use of the lock-in amplifier to measure the photovoltage.

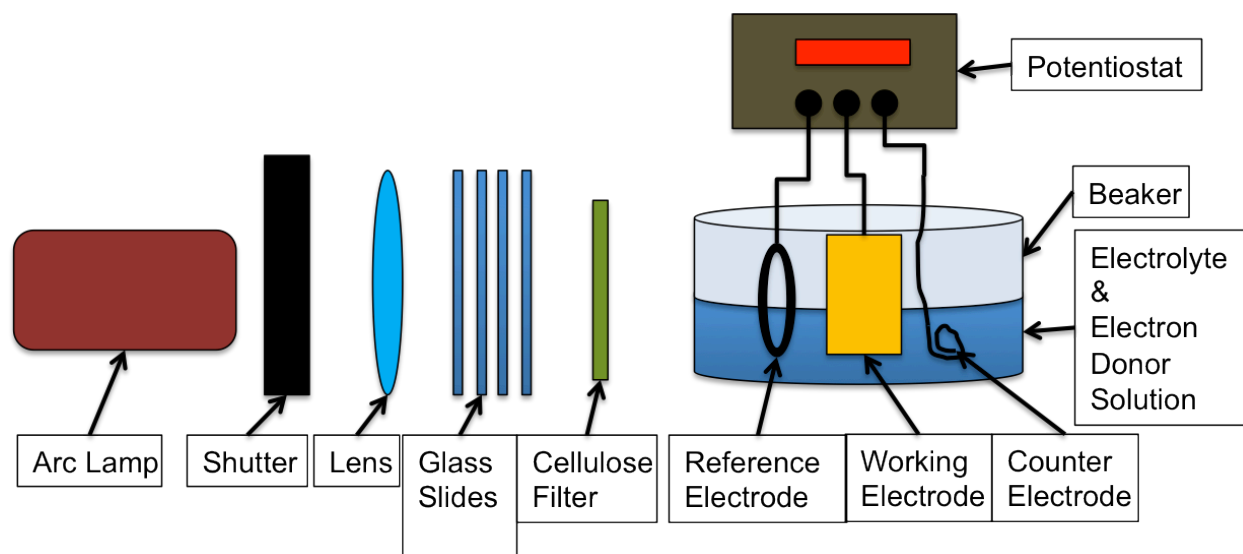


Figure 40: Schematic of potentiostat set-up for measuring photocurrent and photovoltage of the solar cells.

3.5.3 Three Electrode Potentiostat Set-up

In theory, potentiostats only require two electrodes to make measurements of voltage and current in solution. One electrode is the sample under investigation called the working electrode, and the other is the reference/counter electrode used to complete the circuit. However, it is very difficult to maintain the potential of a solution with a reference electrode when there are large currents passing through it. To mitigate this problem, a three-electrode setup is often used with a reference electrode used to hold the potential of the solution, and a counter electrode used to carry current to complete the electrochemical circuit. This way only small currents pass through the reference electrode, and it can more effectively control the potential of the system. Gamry Instruments describes the function of a three electrode setup and reference electrodes well on their website (Gamry Instruments, 2010). Figure 41 below shows the circuit in schematic.

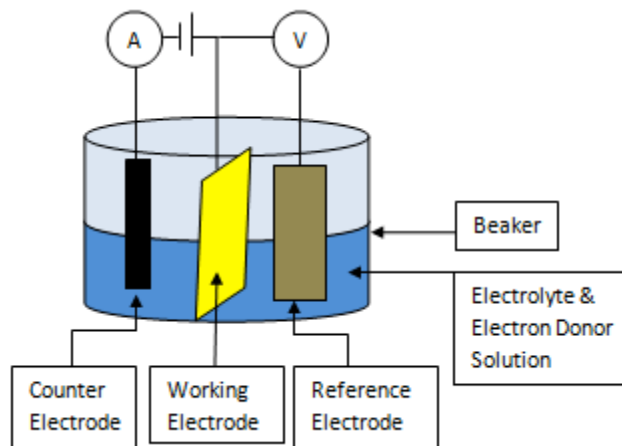


Figure 41: Three electrode setup for measuring potential or current through the solution in an electrochemical experiment. The current carried through the counter electrode and measured with the ammeter A, while potential is compared through the reference electrode and measured with the voltmeter V. The working electrode is the sample under investigation.

3.6 Surface Characterization

Contact angle measurements are made by very carefully placing a drop of water on the surface of a sample and using both high resolution camera and computer software to determine the angle at which the drop of water forms a meniscus. This gives a comparison between what is currently on the outer most surface of a sample by allowing measurement of how hydrophobic or hydrophilic it is. The determination of the angles only gives a benchmark to determine if the surface characteristics have changed and the attachment of further layers of molecules has indeed taken place successfully. The values ranged from 27° to 71° .

The Ultraviolet-Visible spectrophotometer is a device that measures the absorbance or transmittance of differing wavelengths of light when they illuminate a sample. The device can be measure either a solution, or a solid sample. In the case of this experiment the UV-Vis system was used to determine the absorbance of the porphyrin onto the cell. Since the porphyrins that

have a peak absorbance of around 435nm, when the cells were measured a peak in light absorbance was observed near this wavelength. In order to take an absorbance comparison first a sample must be placed in the device that lacks the component that the sample has, this first reading acts as a baseline reading to compare further samples against. A gold slide with only MUA attached to the surface was first placed in the device and measured for a baseline reading, This baseline is only used give an initial comparison, for more accurate absorbance the baseline of the final scan should be checked by hand drawing and measurements of the absorbance peak difference. A sample with MUA and porphyrin attached was measured. See Figure 42 for a diagram of the mechanism.

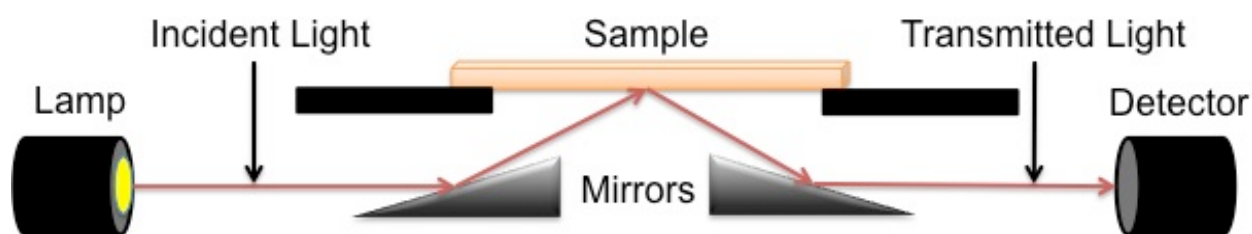


Figure 42: The Ultraviolet visible spectrophotometer works by reflecting light onto a sample and then measuring the amount of light that is detected at different wavelengths.

In order to read the increase of absorbance a sloping baseline must be accounted for. As seen in Figure 43 a baseline should be drawn, the increase in absorbance should be measured from the drawn baseline to the peak at the desired wavelength. The absorbance is calculated with Equation 1. This only gives a relative absorbance; Absorbance is unitless.

$$A_{\lambda} = \ln(I_0/I)$$

Equation 1

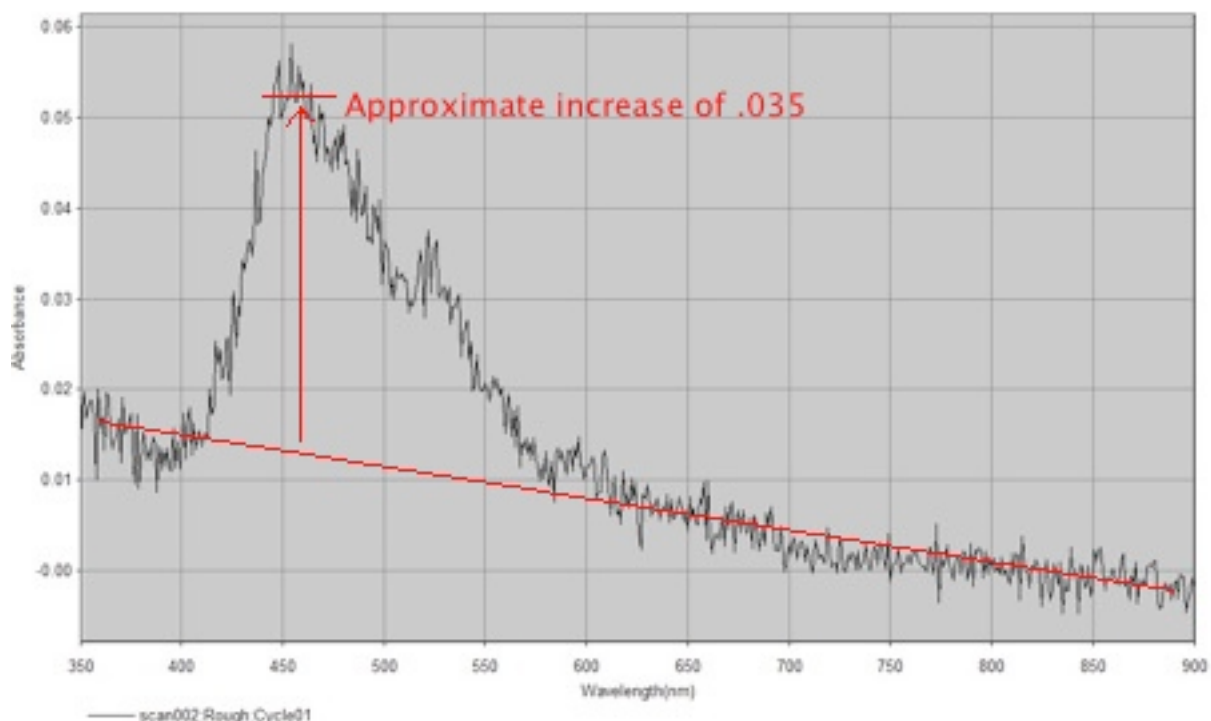


Figure 43: Example absorbance spectra of rough SAM vs. plane gold baseline from 350 nm to 900 nm.

3.7 Atomic Force Microscopy

Atomic force microscopy (AFM) uses a very small probe to measure surface characteristics by scanning the tip along the surface. A common analogy to this is the process of dragging your fingers along a wall to find the light-switch in a dark room. In this analogy you are using your finger as a probe tip to measure the topography of the wall surface. The probes used in AFM have a very fine tip protruding from the end of a cantilever, as seen in Figure 45. To measure the position of the cantilever a laser is shown on the back of the cantilever, and reflected onto a photodiode. The diode is broken into four sections so that the position of the laser on the diode can be measured. In this project intermittent contact mode to measure the surface topography of the solar cells under investigation. In this mode the cantilever oscillates so that the tip repeatedly taps the surface, rather than dragging the tip along the surface.

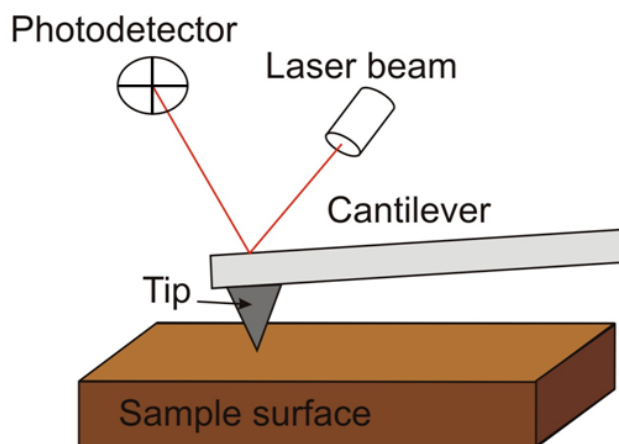


Figure 44 – Schematic of AFM. The tip contacts the surface of the sample, and follows its topography. The height of the cantilever is measured by the location of the laser on the photodiode after it reflects off of the back of the cantilever. (<http://cnx.org/content/m22326/latest/graphics7.jpg>)

Images of the surface of the solar cells were obtained with an Asylum Molecular Force Probe (MFP) atomic force microscope to characterize the roughness of the surface. The microscope was operated in tapping mode to provide high resolution images and to minimize damage to the surfaces. Tap 300 series probes from Budget Sensors [Sofia, Bulgaria] were used for the imaging.

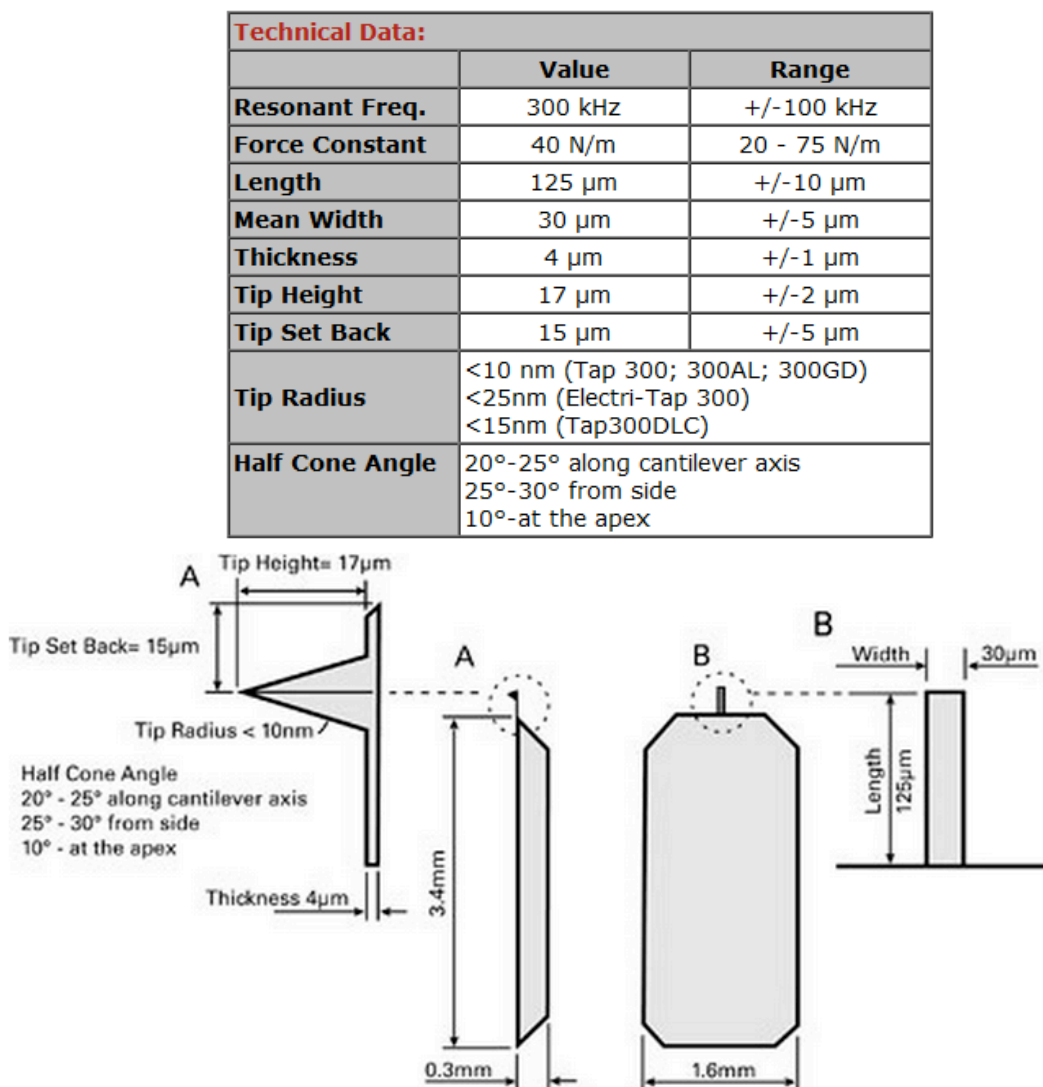


Figure 45 – Specifications for the AFM cantilever and tip used for characterization of the topography of the smooth and rough surfaces (http://www.tedpella.com/probes_html/budgetsensors-1.htm#TAP300all).

For consistency between samples, a standard set of scanning parameters was used. Images were taken at three different scan sizes, 25 μm , 5 μm , and 1 μm with corresponding scan rates of 0.2 Hz, 0.5 Hz, and 1 Hz respectively. The length and width of the nanoparticles on the rough solar cells was approximately 200 nm, so these scan sizes provided: a big picture of the surface to account for any macroscopic variations, a detailed image of the typical surface

features, and a nanoscale zoom of the surfaces to investigate any nano-features glossed over by the larger scan sizes, respectively. Faster scan rates than those specified produced streaking that obscured the image, slower scan rates did not produce significantly improved images. Scan points and scan lines were always 256, an industry standard for providing sufficient resolution without excessively long scan times or excessively large image files. The set point was 800 mV, the Asylum standard for tapping mode. Integral gain was 4.25 and proportional gain 1.00. The gain determines the strength of the negative feedback control circuit. Gain that is too high will cause the instrument to overcompensate when a feature is encountered, which causes oscillation in the height measurement. Gain that is too low causes streaking because the AFM does not respond timely to changes in the topography. Comparing topography measured along a single line by forward and reverse can see this. If the gain is too low, they will not match. As such, the chosen gain values provided the best match between forward and reverse scans for the samples under consideration, without causing any oscillation in the height measurement.

The Asylum AFM has a feature, which measures the effective surface area (total surface area) of the topography, and compares this to the geometric surface area (the planar surface area). To calculate the effective surface area, the software creates a square plane between each set of four points and sums the area of all the squares. This differs from the geometric surface area, which is equivalent to the area of each of these squares one would see from a top down view of the surface. The percent increase in the surface area is the quotient of the effective surface area and the geometric surface area, multiplied by 100%, with 100% subtracted from this result.

References

- Driscoll, P. F., Douglass Jr, E. F., Phewluangdee, M., Soto, E. R., Cooper, C. G. F., MacDonald, J. C., *et al.* (2008). Photocurrent generation in noncovalently assembled multilayered thin films. *Langmuir*, 24(9), 5140-5145.
- Gamry Instruments. (2010). Potentiostat primer.
- Gratzel, M. (2003). Dye-sensitized solar cells. *Journal of Photochemistry and Photobiology*, , 145.
- Wei, Z., Mieszawska, A. J., & Zamborini, F. P. (2004). Synthesis and manipulation of high aspect ratio gold nanorods grown directly on surfaces. *Langmuir*, 20(11), 4322-4326.
doi:10.1021/la049702i

Chapter 4. Results & Discussion

4.1 Results

In this section we outline the results of measurements made to: characterize the porphyrin we used, confirm each step in the synthesis of the solar cells, compare the effective surface area of the smooth and rough surfaces, and compare the ability of the smooth and rough surfaces to generate photocurrent and photovoltage. There is also a section on suggestions of future work at the end. Two batches of cells were made in an attempt to demonstrate repeatability of our method, labeled Batch 1 and Batch 2.

4.1.1 Light Absorbance

The absorbance spectrum for porphyrin in solution was measured because it provides a much clearer spectrum than absorbance measurements made of a surface with a monolayer of porphyrin adsorbed to it. The results show a Soret band at 420 nm and four Q bands at 520, 540, 580, and 640 nm, as seen in Figure 46.

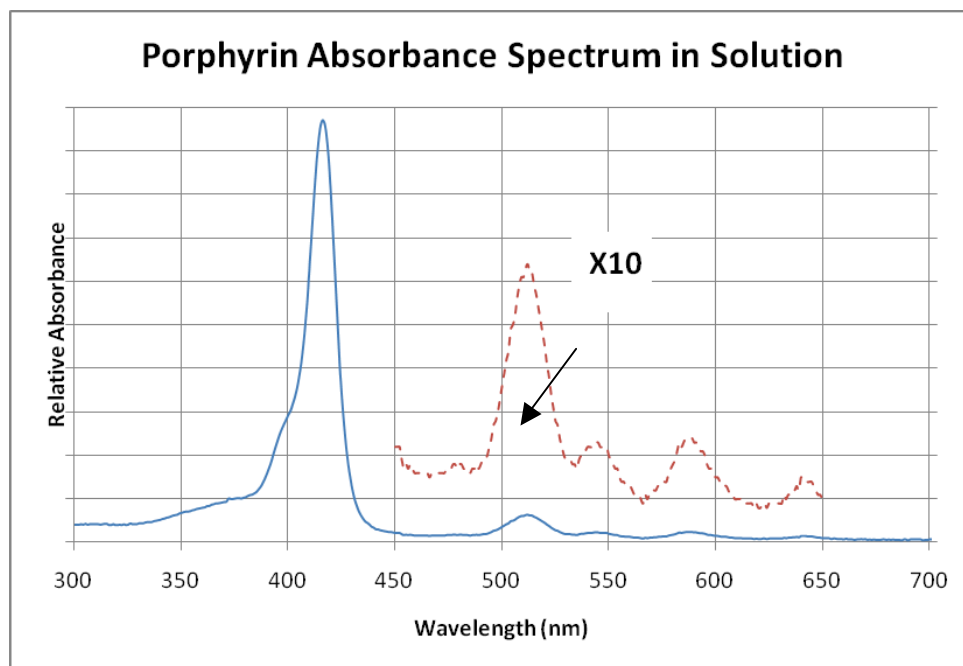


Figure 46: Absorption spectrum of porphyrin. Red shows a magnified section of the spectrum from 450nm to 650 nm for clarity.

The absorbance spectrum for porphyrin adsorbed to the rough and smooth gold surfaces is shown in Figure 47. This was measured to determine what substances on the surface absorb irradiation, and to compare the absorption of the smooth and rough gold surfaces.

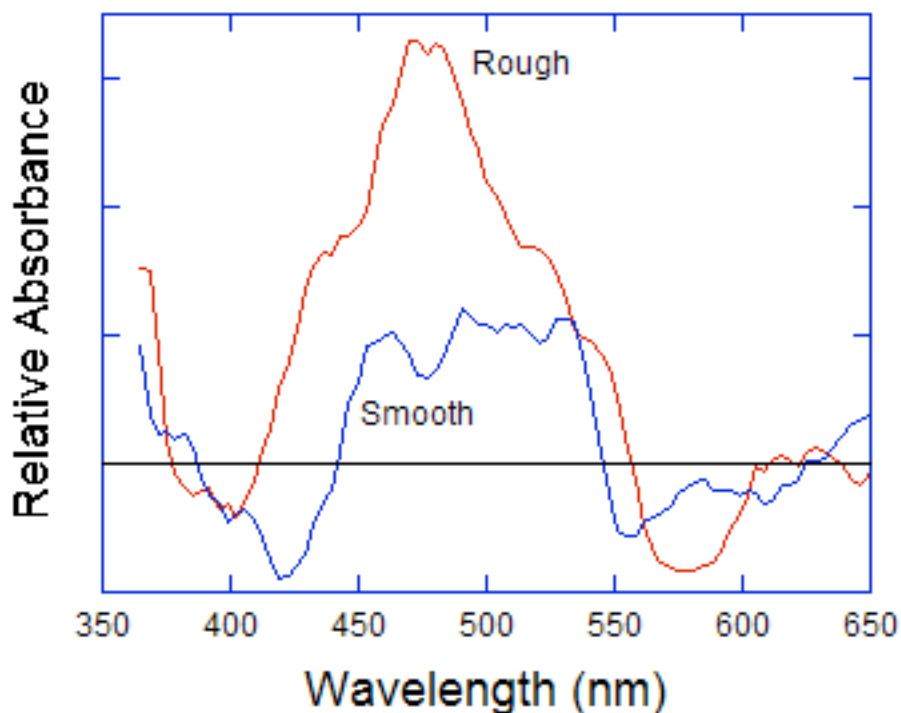


Figure 47: Graph of light absorbance spectrum from 350 nm to 700 nm with a bandwidth of 20nm. This graph is heavily averaged because the raw data were noisy; the measurements were of a monolayer (smooth surface) or a few monolayers (rough surface), which have very low absorption because they are so thin.

4.1.2 Contact Angles

To confirm the presence of MUA, Porphyrin, and gold nano-particles on the gold slides, contact angle measurements were made of the surfaces at each step of the synthesis process. The angles demonstrate a difference in the cells for each step of their synthesis: both for attachment of the gold nano-particles and for attachment of the SAM molecules.

Contact Angle Measurements in Degrees						
Batch 1						
Sample:	Smooth Gold	Smooth MUA	Smooth Porphyrin	Rough Gold	Rough MUA	Rough Porphyrin
	40.7	41.5	26.7	62.4	49.9	49.5
	32.7	40.5	29.3	65.6	51.1	36.4
	31.9	34.5	27.9	66.8	57.7	40.6
	34.1	35.7	31.0	71.0	58.0	34.5
	35.4	34.2	37.6	63.2	52.3	35.1
				60.9	53.2	40.1
Averages:	35.0	37.3	30.5	65.0	53.7	39.4
Standard Deviation:	3.5	3.5	4.3	3.6	3.4	5.6

Table 2: Contact angle measurements were made of each slide for each step in their synthesis. This table shows the original measurements and the averages and standard deviation for each step of the cells produced in Batch 1.

Contact Angle Measurements in Degrees						
Batch 2						
Sample:	Smooth Gold	Smooth MUA	Smooth Porphyrin	Rough Gold	Rough MUA	Rough Porphyrin
	37.4	62.6	59.0	34.2	58.5	61.5
	34.8	60.1	65.5	35.7	55.7	61.9
	39.0	63.2	67.9	30.9	53.2	60.3
	28.3	62.3	54.8	36.0	51.2	39.9
	33.2	61.3	54.0	36.7	50.7	40.4
	36.3	66.5	57.0	34.5	59.8	53.6
Averages:	34.8	62.7	59.7	34.7	54.9	53.0
Standard Deviation:	3.8	2.2	5.7	2.1	3.8	10.0

Table 3: Contact angle measurements of Batch 2.

4.1.3 Filtering the Irradiation

To confirm that the photovoltage (PV) and photocurrent (PI) is generated by the porphyrin, and not other chemicals or the photoelectric effect, irradiation of wavelength shorter than 481 nm and 340 nm was filtered out, respectively.

Tests with Filters and Phasing						
<i>Cell</i>	<i>PV (uV)</i>	<i>PI (nA)</i>		<i>Cell</i>	<i>PV (uV)</i>	<i>PI (nA)</i>
NS1	0.252	0.218		NR1	0.230	0.355
<i>with 340+ nm filter</i>	0.185	0.166		<i>with 340+ nm filter</i>	0.162	0.295
<i>with 481+ nm filter</i>	0.003	0.016		<i>with 481+ nm filter</i>	0.011	0.075
S2	0.660	0.680		R1	1.060	1.050
<i>with 340+ nm filter</i>	0.150	0.160		<i>with 340+ nm filter</i>	0.900	0.980
<i>with 481+ nm filter</i>	0.760	0.640		<i>with 481+ nm filter</i>	0.364	0.320

Table 4: Measurements taken of the cells with different filters. The 340 nm filter cuts out Ultra Violet light showing that very little PV and PI are produced with this wavelength. The 481 nm filter demonstrates that a majority of PV and PI is produced by wavelengths of light absorbed by porphyrins, indicating that the porphyrins are responsible for the photoelectric effect in our samples.

4.1.4 Photobleaching

To determine solar cells' consistency of photovoltage and photocurrent over time, a photobleaching test was done. Periodically the irradiation was blocked with the shutter to confirm the zero had not shifted. Figure 48 shows the results of a bleaching test done on a smooth gold surface with porphyrin.

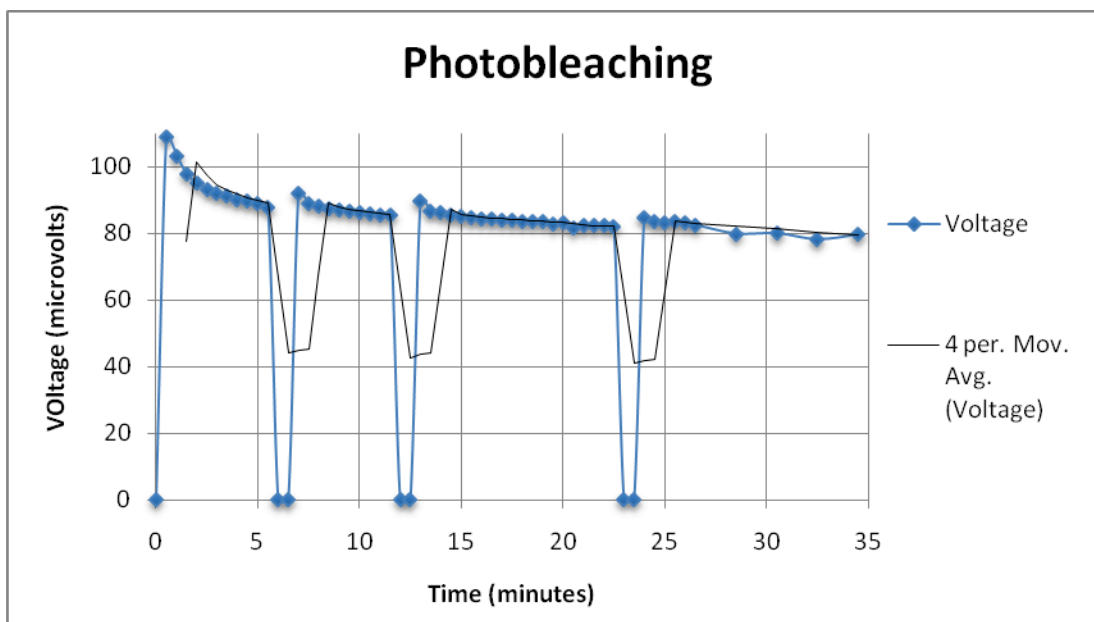


Figure 48: Photo bleaching shows a relatively slow decline of voltage with time, measurements were not taken to a full half-life though so full bleaching would be difficult to estimate. At three intervals the light source was covered in order to test the zero of the reading

4.1.5 AFM Topography

The smooth and rough surfaces for each batch were characterized with Atomic Force Microscopy (AFM). The images below in Table 5 and Table 6 show the topography of a sample cell from each batch of smooth and rough cells. These cells were bare gold, meaning there was no monolayer deposited on them. An image was taken for each stage of the nano-particle deposition process, the smooth gold surface, the surface with gold seed particles on it, and the surface after the nano-particles had been grown from the seeds, which was the final rough surface. Table 6 also shows the effective surface area, and percent increase of the effective surface compared to the geometric surface area.

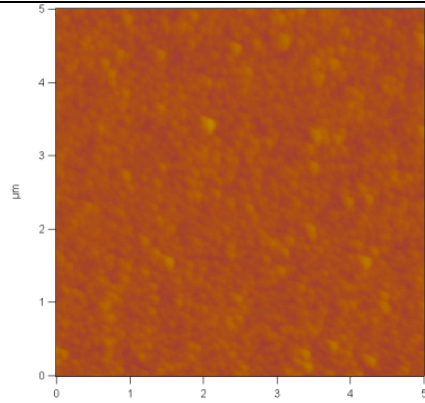
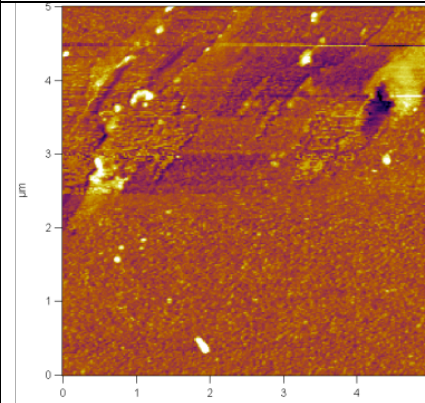
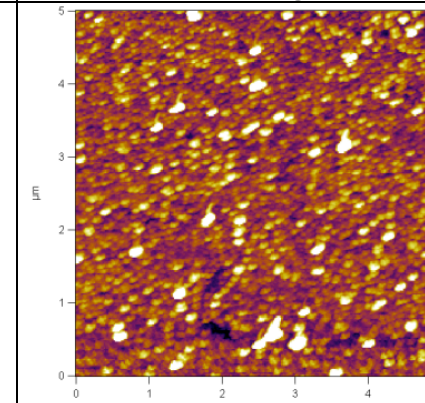
Batch 1 AFM images and Information		
Smooth	Seed	Rough
		
Surface Area: 25.0 μm^2	Surface Area: 25.4 μm^2	Surface Area: 26.2 μm^2
Area Percent: 0.07 %	Area Percent: 1.71 %	Area Percent: 4.94 %

Table 5: From left to right AFM images of smooth surface, smooth surface with seed particles attached, surface with grown gold nano-particles. These images and statistics are from Batch 1.

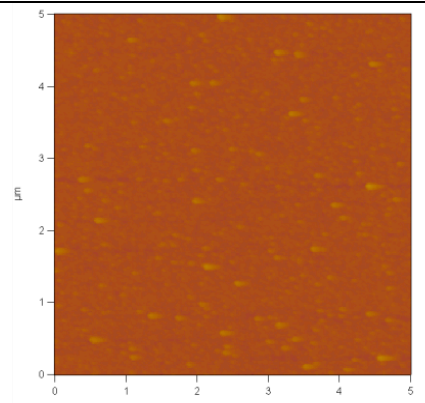
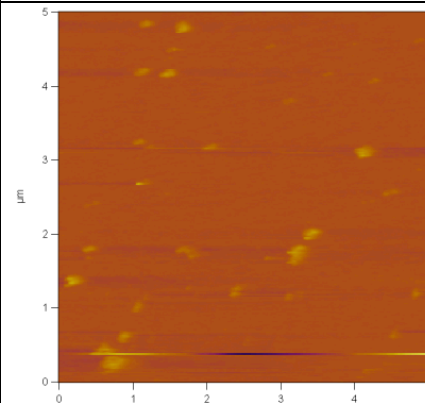
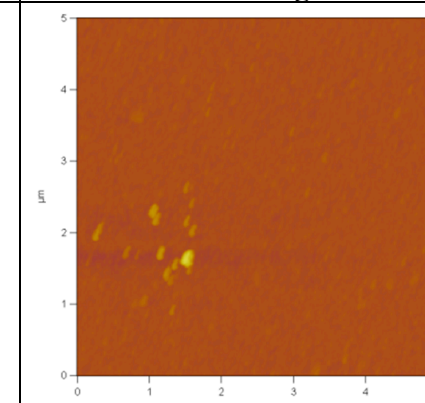
Batch 2 AFM images and Information		
Smooth	Seed	Rough
		
Surface Area: 25.2 μm^2	Surface Area: 25.1 μm^2	Surface Area: 25.3 μm^2
Area Percent: 0.64 %	Area Percent: 0.40 %	Area Percent: 1.02 %

Table 6: AFM images of the smooth gold surface, gold seed particle surface, and rough gold nano-particle surface from Batch 2. The seed particle surface is created from a smooth surface, and the gold nano-particles are then grown from these seeds.

4.1.6 Photovoltage and Photocurrent

The difference in the ability of the smooth and rough cells to produce PV and PI was determined by measuring each cell and averaging all the measurements for each type of cell in each batch. The percent increase was calculated as

$$\% \text{ increase} = \frac{(\text{Rough}_{\text{ave}} - \text{Smooth}_{\text{ave}})}{(\text{Smooth}_{\text{ave}})} * 100\%$$

These measurements for Batch 1 showed a 56% increase in PV and a 63% increase in PI. Batch 2 showed a 35% decrease in PV and a 39% increase in PI. The data are shown below in Tables Table 7 and Table 8.

Batch 1					
Smooth			Rough		
<i>Cell</i>	<i>PV (uV)</i>	<i>PI (nA)</i>	<i>Cell</i>	<i>PV (uV)</i>	<i>PI (nA)</i>
s1.2	0.71	0.50	r1.2	1.06	1.05
s2.2	0.66	0.68	r1.2 - 340	0.9	0.98
s3.2	0.55	0.51	r3.2	0.95	0.89
s4.2	0.64	0.56	r4.2	0.92	1.14
s5.2	0.80	0.92	r5.2	1.18	1.13
<i>Average:</i>	0.67	0.63	<i>Average:</i>	1.05	1.03
<i>Standard deviation</i>	0.09	0.18	<i>Standard deviation</i>	0.12	0.11
<i>% change PV</i>	56% ± 14%				
<i>% change PI</i>	62% ± 28%				

Table 7: Photovoltage (PV) and Photocurrent (PI) of the smooth and rough cells from Batch 1.

Batch 2					
Smooth			Rough		
<i>Cell</i>	<i>PV (uV)</i>	<i>PI (nA)</i>	<i>Cell</i>	<i>PV (uV)</i>	<i>PI (nA)</i>
NS1	0.252	0.218	NR1	0.230	0.355
NS2	0.127	0.202	NR2	0.134	0.358
NS3	0.102	0.271	NR3	0.178	0.315
NS4	0.326	0.315	NR4	0.07	0.169
NS5	0.53	0.109	<i>Average:</i>	0.153	0.299
NS6	0.081	0.209	<i>Standard deviation:</i>	0.067	0.089
NS7	0.234	0.144			
NS8	0.197	0.22			
NS9	0.431	0.198			
NS10	0.093	0.260	<i>% change PV</i>	-36% ± 64%	
<i>Average:</i>	0.237	0.214	<i>% change PI</i>	39% ± 30%	
<i>Standard deviation:</i>	0.152	0.059			

Table 8: PV and PI measurements of smooth and rough cells from Batch 2.

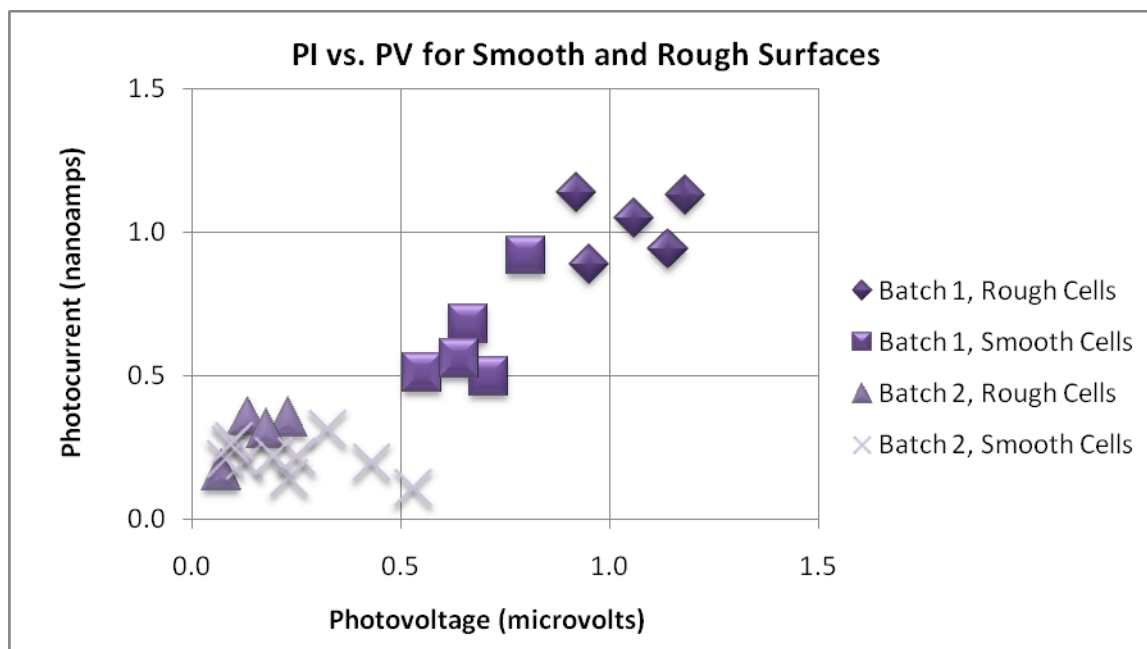


Figure 49: This plot provides a convenient means of seeing the trends of photovoltage and photocurrent simultaneously. There was only a slight increase in the photovoltage for the rough cells in Batch 2, compared to the smooth cell in Batch 2. However, both the photovoltage and photocurrent increase significantly for the rough cell in Batch 1, compared to the smooth cells in Batch 1. This is consistent with measurements of the topography.

4.2 Discussion

This section discusses the results to determine their significance and what correlations exist between each method of characterizing the photovoltaic electrodes.

4.2.1 Light Absorbance

The measurement of the absorbance spectrum of the porphyrin on the smooth and rough gold surfaces, shown in Figure 47, helps determine two things: which substances are absorbing irradiation, and how much of the incident light is absorbed by the surface. Comparing this spectrum to the absorbance of the porphyrin in solution, we see the same characteristic Soret

band at 420 nm. This peak is slightly shifted and broadened, which is expected because the porphyrin is dry and bound to the monolayer rather. This suggests that the majority of the absorbance of the gold slides is done by the porphyrin, and not the MUA or the gold.

Comparing the absorbance spectrum of the smooth and rough surfaces, we see that the rough surface has a higher absorbance than the smooth surface. This suggests that the rough cell will perform better as a photovoltaic. However, it is possible that side reactions introduced by the topography of the rough cell could prevent this absorbed energy from generating charge separation. Measurement of the PV and PI is necessary to confirm how the rough cell performs as a photovoltaic.

4.2.2 Contact Angles

Sharma *et al.* (Sharma, Broker, Szulczewski, & Rogers, 2000) measured the contact angle of MUA on smooth gold to be 28° and with porphyrin added to be 38° . The low angle of 28° was as expected, due to the hydrophilic nature of the acid terminated MUA. The 38° angle is also as expected, due to the hydrophobic nature of porphyrin. This makes our measurements interesting because they start at a much higher angle, anywhere from 37° to 63° , and consistently decreased with the addition of the porphyrin.

In Batch 1, the rough surface had a much higher contact angle than the smooth surface, which is as expected as rough surfaces tend to be hydrophobic.

Batch 2 showed no significant difference between the smooth and rough surfaces. Comparing the contact angle of the bare gold for the rough and smooth surfaces in Batch 1 and 2, there is indication that there was no nano-particle growth on the rough surface of Batch 2.

4.2.3 Filtering the Radiation

As shown in Table 4, the 481 nm filter substantially decreased the PV and PI output of the cell. This was expected since the main absorption band for porphyrin is between 350 nm and 480 nm, demonstrated by the 420 nm Q band in Figure 46 and Figure 47. The 340 nm filter made little difference in the PV and PI, which confirms that the photoelectric effect, activated by light of wavelength shorter than 340 nm, is not a substantial source of PV and PI.

4.2.4 Photobleaching

The results shown in Figure 48 demonstrate that, despite an initial drop off, the PV and PI are very stable over a period of 30 minutes. Since all the measurements of PV and PI require only a few minutes each, and only a few measurements must be made of each cell, bleaching of the cells over time does not need to be considered when analyzing our data.

4.2.5 AFM Topography

Height measurements are very accurate in AFM, but the width measurements can be distorted if the AFM tip is wider or less steeply sloped on its side than the side of the features under observation. There can also be open spaces underneath objects, which the AFM tip will not be able to reach and thus cannot characterize when measuring the topography of a surface. These phenomena are shown for spherical gold nano-particles on a smooth gold surface by an illustration in Figure 50. All of these surfaces, which the AFM tip cannot reach, may provide surface area onto which the porphyrin monolayer could adsorb. As such, AFM measurements of how much the effective surface area increases with the addition of gold nano-particles is a lower limit of how much more surface the nano-particles actually provide.

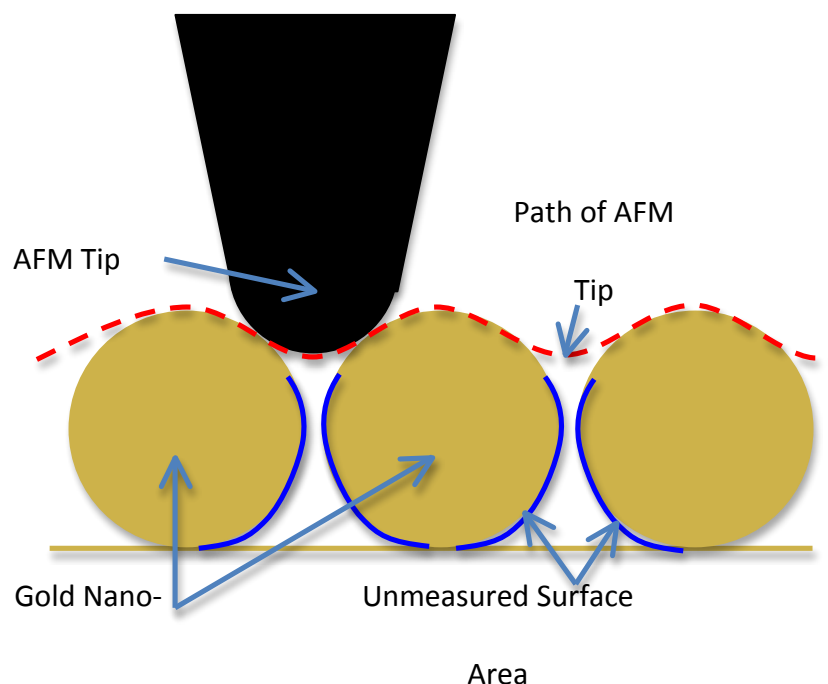


Figure 50: AFM allows for accurate height measurements but can introduce error in width measurements if the width of the tip is comparable to that of the features being characterized. There can also be regions of the topography which the tip cannot reach. This is demonstrated above for a surface with spherical gold nanoparticles.

Two different mathematical models were used to predict the potential increase in surface area from adding the gold nano-particles to the smooth gold substrate. The two models, depicted in Figure 51, assume that the nano-particles are spherical in shape. The first model assumes that half of the surface is covered with spherical nano-particles. The second model assumes that the entire surface is covered with hemispherical nano-particles. The second model is more likely than the first because the size of the nano-particles is much greater than the distance of the gold seed particle from the smooth gold substrate so it is likely that the particles would grow as hemispheres. From the equation for the surface area of a sphere, $SA = 4\pi r^2$, the results in Table 9 were determined.

Particle Shape	Particle Radius (nm)	Smooth SA (μm^2)	Rough SA (μm^2)	Percent Increase
Sphere	100	25	64.3	157.0
Hemisphere	100	25	44.6	78.5

Table 9: Shown here is the predicted surface area for the rough nano-particle surface, corresponding to the mathematical models depicted graphically in Figure 51.

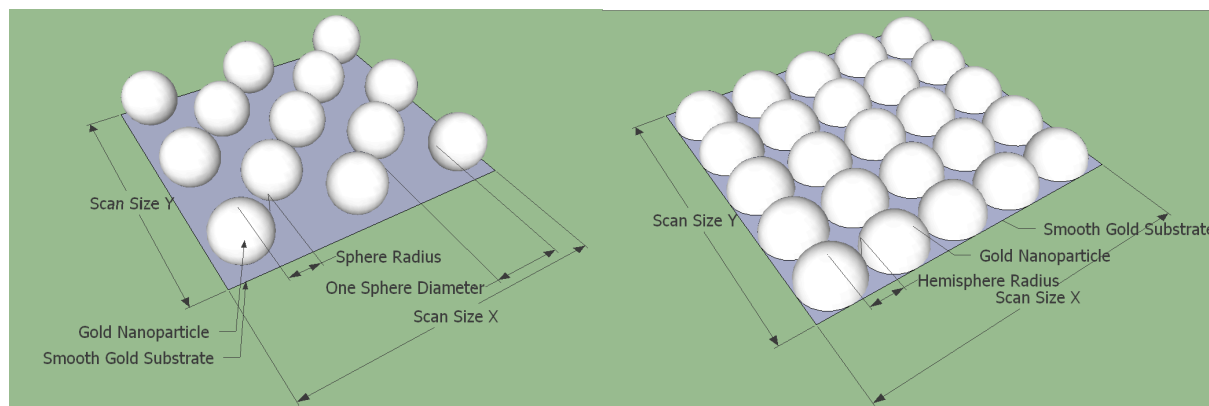


Figure 51: Two mathematical models of potential idealized surfaces of the gold substrate when roughened with gold nano-particles. The image on the left is the first model showing a surface half covered in spheres, and the image on the right the second model showing a surface completely covered in hemispheres.

In Batch 1 there is a distinct difference between the smooth surface and the surface following deposition of the seed particles, which suggests that the seed particle deposition was effective. The nano-particle growth shows even more change suggesting that the growth process was also effective. The increase in surface area went from 0.07% for the smooth surface to 4.94% for the nano-particle growth, showing a marked increase in effective surface area; the ultimate objective of adding the nano-particles. As described previously, this measurement of surface area is a lower limit, and the increase in surface area with the addition of the gold nano-particles is likely much greater than 5%. This is in agreement with contact angle measurements.

Surface topography measurements in Batch 2 showed little difference between the smooth, seed, and rough surfaces. This suggests that the process was not effective, which is also consistent with the contact angle measurements. This also suggests that there will not be a difference between the photovoltage and photocurrent produced by the smooth and rough surfaces in Batch 2.

4.2.6 Photocurrent and Photovoltage

Batch 1 showed an increase in photovoltage and photocurrent, which is consistent with the AFM topography measurements and the contact angle measurements. The large increase of about 50% is a factor of 10 larger than the increase in surface area measured by AFM, which suggests that there may indeed be more surface area added to the surface by the nano-particles than the AFM can measure. The standard deviation of the increase in surface area is large, but raises no question that there was a marked increase in photovoltage and photocurrent for the rough cell in comparison to the smooth cell.

Batch 2 showed no noteworthy increase in photovoltage or photocurrent when comparing the smooth and rough gold cells. It actually showed a decrease in photovoltage and a slight increase in photocurrent, but with double the standard deviation and equivalent to the percent change, respectively. This is consistent with the AFM topography measurements and the contact angle measurements for Batch 2, which showed little difference between the smooth and rough surfaces. The decrease, though not very statistically significant, is one area of possible future investigation.

The magnitude of the photovoltage and photocurrent produced by these cells is very small, considering that a 420 nm photon has enough energy to impart 2.9 V onto an excited electron. Indeed, if there was excellent coverage of porphyrin molecules on the surface and they

were all absorbing photons to create charge separation our potential would be on the order of volts. However, because the film is thin there are not many porphyrin molecules per unit area. Also, not all excitation energy is converted to charge separation, and there is often recombination of charges between the porphyrin and electrolyte. These factors reduce the net charge separation that occurs, resulting in microvolts between the primary and counter electrode. Likewise, because so little charge is transferred to each electrode, the photocurrent is very low, on the order of nanoamps.

Chapter 5. Summary & Recommendations

5.1 Summary

These results suggest that the addition of gold nano-particles to a smooth gold substrate seems to substantially increase the performance of organic solar cells. This offers an inexpensive and simple approach to improving the cells, which offer a promising alternative to silicon photovoltaics.

5.2 Recommendations

5.2.1 Improving the Gold Nano-Particle Rough Surface

There is much more work to be done to confirm that the addition of nano-particles increases the photovoltage and photocurrent of thin-film solar cells and to fully characterize and optimize the system. This will involve fully characterizing the topography of the surface, understanding how the topography affects the photovoltage and photocurrent, and optimizing the rough surface accordingly. There was only time to create two batches of smooth and rough surfaces, the second of which was unsuccessful. The creation of the rough surfaces is more an art than a science, so experience should allow for more consistent production of the rough surfaces. However, demonstrating this repeatability and determining whether these rough surfaces consistently produce a 50% increase in photovoltage and photocurrent will be an important first step.

If the effectiveness of adding nano-particles is confirmed there are several techniques that can be used to better characterize the topography. Electrochemical measurements can be made of the capacitance of the smooth and rough surfaces, which indicate the surface area since

capacitance is proportional to surface area. The surface area can also be measured by adsorbing molecules onto the surface and subsequently desorbing them into solution. By measuring the concentration of the molecules in solution the surface area can be determined. AFM can also be used to better understand the surface. For example, to determine how thick the nano-particle layer is a mask can be laid on the smooth gold throughout the synthesis of the nano-particles. Removing the mask will provide the AFM a zero reference from which to measure the height of the nano-particles.

Changing the topography of the surface raises a number of questions about how porphyrin molecules absorb light and where the excitation energy goes afterwards. Regarding light absorption, porphyrin is a planar molecule and thus has orientation factors associated with the absorption of light. This could be investigated through experiments involving polarized light to understand how the topography affects the orientation factors of the porphyrin. Regarding the path of excitation energy, the rough surface could potentially disrupt the structure of the monolayer and cause the energy to never produce a charge separation. This disruption could also cause recombination of charge between the electrolyte and the thin film and thereby reduce the photovoltage and photocurrent. This could be investigated by measuring the absorption of the thin-film and comparing it to the generation of photovoltage and photocurrent by smooth and rough electrodes. This will show if the rough topography causes any change in the efficiency by which absorbed photons are converted to photovoltage and photocurrent.

Controlling the nano-particle surface topography will allow the surface to be optimized for maximum power output of the solar cell. Since the gold nano-particles are grown on a gold substrate, there may be growth of gold between the nano-particles, reducing the increase in surface area. If this happens spacer molecules could be included in the linking molecule

monolayer, which could prevent gold growth between nano-particles. Variation of the growth solution could also affect the size and shape of the nano-particles. A number of other variables in the synthesis process of the nano-particle rough surface could also be changed to modify the topography of the nano-particle surface and optimize it for maximum power generation.

5.2.2 Developing a Commercially Viable Solar Cell

This method for improving incident photon to current efficiency of a thin-film organic solar cell electrode by adding gold nano-particles to the electrode surface is informative, but cannot lead directly to the development of a competitive solar cell in today's marketplace. To produce a competitive solar cell will require increasing the cell's power output by approximately a factor of 1000. Such an increase will require a creative solar cell design that either further modifies the electrode, or arranges the electrode in a strategic manner.

To improve the absorption of the thin-film, a multilayered film could be used. Driscoll *et al.* demonstrated that films with multiple layers of dye molecules were able to produce substantially more power output than films with a single layer of dye molecules (Driscoll *et al.*, 2008).

One approach to cell construction is to include many layers of the self-assembled monolayer (SAM) coated electrodes stacked vertically one on top of another. Using indium-tin oxide coated glass, which is transparent, instead of gold coated glass would allow for incident light to be absorbed by multiple layers of the SAM coated electrodes.

The SAM coated electrodes could also be stacked horizontally. This way the gold substrate, which is cheaper than indium-tin oxide, could still be used (Jalbuena 2011). The incident light would travel the length of the monolayer in this arrangement, effectively increasing the thickness of the layer of dye molecules by many orders of magnitude.

Another possibility is the extension of nano-tubes from the surface, which could then be roughened with gold nano-particles as done in this report for a flat surface. This would allow for an even greater increase in the surface area of the electrode, which could potentially provide the increase in absorption necessary to make the cell commercially viable.

The addition, small 5 nm diameter nano-particles could be added to the surface to improve the transfer of excitation energy from the excited dye molecules to the heterojunction at which charge separation takes place. These small nano-particles have been shown by Rand *et al.* to increase the absorption of thin-film solar cells, and could add a finer level of surface modification to our present method and those discussed above (Rand, Peumans & Forrest 2004).

Increasing the efficiency by which the excited electrons are injected into the electrolyte or semi-conductor could also address this problem. Research could be focused on the development of a very efficient electrolyte solution that could match the excitation energy levels of a given dye (Giannoulli *et al.*, 2010). If this was done then excitation energy would flow more easily from an excited dye molecule into the electrolyte solution. It is also possible that this could be accomplished by creating a solid semiconductor that matched the excitation energy levels of the dye.

A Schottky barrier could be built by layering thin amounts of different metals onto the electrode (Ji *et al.*, 2005). This could improve the efficiency of converting excitation energy to charge separation by reducing the amount of charge recombination.

These approaches could be combined to build a nano-tube surface roughened by gold nano-particles on either a gold or an indium-tin oxide substrate. The electrode could have a film with multiple layers of dye molecules. Small nano-particles could be added to help facilitate charge transfer from the SAM to the electrolyte, and a titanium oxide layer and a Schottky

barrier could be built onto the top of the electrode to prevent charge recombination. An appropriate electrolyte could be chosen to further enhance the efficiency of the excitation energy transfer to the charge separation. The electrodes could be stacked either vertically or horizontally, depending on the choice of substrate, to improve absorption of the incident light.

The layers of metal in the Schottky barrier can only be a few nanometers thick before the efficiency begins to drop drastically. Also, the order of the structure of the film with multiple layers of dye molecules would likely be sensitive to the roughness of the surface, potentially falling apart for too rough a surface. Consequently, this approach of combining many different strategies would need to balance the size of the nano-tubes and nano-particles with preserving the structure of the Schottky barrier and the multilayered film. Future work could attempt to find the maximum size of the nano-tube and nano-particle layer before the effectiveness of the Schottky barrier and multilayered film began to decrease significantly.

References

- Sharma, C. V. K., Broker, G. A., Szulczewski, G. J., & Rogers, R. D. (2000). Self-assembly of freebase- and metallated-tetrapyridylporphyrins to modified gold surfaces. *Chemical Communications*, (12), 1023-1024. Retrieved from <http://dx.doi.org/10.1039/B002084M>
- Ji, X., Zuppero, A., Gidwani, J. M., & Somorjai, G. A. (2005). *The catalytic nanodiode: gas phase catalytic reaction generated electron flow using nanoscale platinum titanium oxide schottky diodes*. *Nano Letters*, 5(4), 753-756. doi:10.1021/nl050241a
- Giannouli, M., Syrokostas, G., & Yianoulis, P. (2010). *Effects of using multi-component electrolytes on the stability and properties of solar cells sensitized with simple organic dyes*. *Progress in Photovoltaics*, 18(2), 128-136. doi:10.1002/pip.952
- Driscoll, P.F., Douglass Jr, E.F., Phewluangdee, M., Soto, E.R., Cooper, C.G.F., MacDonald, J.C., Lambert, C.R. & McGimpsey, W.G. 2008, "Photocurrent Generation in Noncovalently Assembled Multilayered Thin Films", *Langmuir*, vol. 24, no. 9, pp. 5140-5145.
- Jalbuena 2011, *Gold is used in cheap electrodes for organic solar cells*.
- Rand, Peumans & Forrest 2004, "Long-range absorption enhancement in organic tandem thin-film solar cells containing silver nanoclusters", *Journal of Applied Physics*, vol. 96, no. 12, pp. 7519-7527.